CHROMITITES OF THE URALS (PART 1): OVERVIEW OF CHROMITE MINERAL CHEMISTRY AND GEO-TECTONIC SETTING

Giorgio Garuti*,✉, Evgeny V. Pushkarev, Oskar A.R. Thalhammer*** and **Federica Zaccarini***

* *Department Angewandte Geowissenschaften und Geophysik, Montanuniversität Leoben, Austria.*
** *Institute of Geology and Geochemistry, Ural Branch of the Russian Academy of Science, Ekaterinburg, Russia.*
✉ *Corresponding author, e-mail: giorgio.garuti@unileoben.ac.at*

Keywords: *Chromitite, overview, chromite mineral chemistry, tectonic setting. Urals.*

ABSTRACT

Published and unpublished compositions of chromite in 333 chromitite samples from 14 ultramafic complexes of the Urals are overviewed. The chromitites occur in the mantle unit and/or the supra-Moho cumulate sequence of ophiolite complexes, as well as in Alaskan-type intrusions. They vary in size from giant ore deposits associated with ophiolites (e.g., Kempirsai, Ray-Iz, Voykar-Syninsky) to sub-economic mineralization in the Alaskan-type complexes (e.g., Svetly Bor, Kachkanar). Mantle-hosted chromitites occur either as discordant, podiform, high-Cr ore bodies and sub-concordant elongated lenses of high-Al chromite. In the supra-Moho sequences of ophiolites, chromitite is mainly of the high-Al variety, and occurs as concordant layers alternated with peridotite and pyroxenite cumulates. In the Alaskan-type intrusions of the Urals, chromitite occurs as centimeter to meter-size pods and lenses having syngenetic or epigenetic relationship with the host dunite.

Calculated melt compositions in equilibrium with chromite and comparison of chromite composition with those from various volcanic suites, and chromitites from different plutonic complexes, allow division of the Urals chromitites into four different compositional groups, corresponding to different geodynamic environments of formation:

1) The high-Al, low-Ti suite (Al_2O_3 > 20 wt%, Cr# < 0.70, av. TiO_2 = 0.15 wt%, av. Fe^{3+}# = 0.05, $\delta logf(O_2)$ = -0.1 ÷ +2.3) includes most of the supra-Moho stratiform chromitites and some podiform chromitites hosted by the ophiolitic mantle rocks. These chromitites crystallized from MORB-type tholeiitic magmas (av. FeO/MgO = 1.0), produced by low degrees of partial melting of a slightly depleted source in subduction-unrelated geodynamic settings.

2) The high-Al, high-Ti suite (Al_2O_3 > 20 wt%, Cr# < 0.70, av. TiO_2 = 0.80 wt%, av. Fe^{3+}# = 0.20) is represented by the CHR-2 chromitite from the supra-Moho cumulus sequence of the Nurali ophiolite complex. The calculated melt in equilibrium with chromite differs from MORB in having higher FeO/MgO = 1.90, while the chromite displays characteristics of spinels in intra-plate basalts and chromitites in layered intrusions. The coexistence of chromitites derived from MORB and transitional tholeiites in the Nurali cumulate sequence is considered a feature typical of continental margin ophiolite complexes.

3) The high-Cr, low-Ti suite (Cr# > 0.70, Al_2O_3 < 20 wt%, TiO_2 < 0.30 wt%, av. Fe^{3+}# = 0.06, $\delta logf(O_2)$ = -1.7 to +2.7) includes most podiform chromitites hosted by the ophiolitic mantle rocks and a few examples of supra-Moho stratiform chromitites. They have crystallized from high-Mg magmas with average compositions referable to picritic tholeiite and boninite (FeO/MgO < 1.0). These chromitites are typically found associated with subduction-related ophiolites of the Urals.

4) The high-Cr, high-Ti suite (Cr# > 0.70, Al_2O_3 < 20 wt%, TiO_2 = 0.38-1.30 wt%, Fe^{3+}# = 0.20-1.29, δ $logf(O_2)$ = +0.9 ÷ +5.9) is represented by chromitites from the Urals Alaskan-type intrusions and the East-Khabarny complex. They have crystallized from Fe-rich magma (av. FeO/MgO = 1.35) under oxygen-fugacity conditions well above the FMQ buffer. The melt is characterized by high-Ti, high-K, calc-alkaline composition, having many geochemical characteristics in common with ankaramites. It was generated by partial melting of a fluid-metasomatized mantle source, in a subduction-influenced arc setting. However, the close similarity with the zoned complexes emplaced in the Russian-Far-East craton suggests that formation of Alaskan-type melts may be not restricted to SSZ, island arc settings.

INTRODUCTION

The Ural Mountains record a long history of exploration and recovery of chromium starting from the beginning of the twentieth century, when the metal was introduced into the stainless-steel industry. Since then, the Urals have supplied almost one half of the world's chromite ore production, becoming the second leader in the chromium market after the Bushveld complex of South Africa (Stowe, 1987; 1994).

World-class chromite deposits of the Urals are restricted to the mantle tectonite of subduction-related ophiolites (Koroteev et al., 1997). However, chromitites varying in size from potential ore deposits down to sub-economic concentrations of chrome spinel also occur associated with various types of ophiolites and Ural-Alaskan type complexes. (Kravchenko, 1986a; 1986b; Kravchenko and Grigoryeva, 1986; Saveliev and Savelieva, 1991; Chashchukhin et al., 1996; 1998; 2002; 2007; Melcher et al., 1994; 1997; 1999; Ivanov, 1997; Garuti et al., 2003; Savelieva, 2004; Zaccarini et al., 2004b; 2008, 2011; Grieco et al., 2007; Pushkarev et al., 2007). Structural and compositional characteristics of the chromitites vary according to the geological setting of the host complexes. In particular, the chromite mineral chemistry reflects the composition of the parental magmas and evolution of their mantle sources, emphasizing the role of chrome spinel as a guide to the tectonic setting of mafic-ultramafic complexes (Irvine, 1965; 1967; Thayer, 1970; Hill and Roeder, 1974; Evans and Frost, 1975; Dick and Bullen, 1984; Roeder and Reynolds, 1991; Arai, 1992; Leblanc and Nicolas, 1992; Roeder, 1994; Zhou and Robinson, 1994; Barnes and Roeder, 2001).

The primary purpose of this paper is to provide the reader with a compilation of electron microprobe analyses of chromite from chromitites associated with different types of ultramafic complexes of the Urals: ophiolite sequences and Ural-Alaskan type intrusions. Compositional variations of chromite in relation with the inferred geological setting of the host complexes have been critically overviewed. Published data on physical parameters in the chromite-forming system (i.e., temperature and oxygen fugacity, fO_2) have also been summarized and compared. As a new contribution, the composition of chromite was used to calculate the possible composition of the silicate melt in equilibrium with crystallizing chromite. Finally, compositions of the Urals chromitites are

compared with spinel compositions from different types of volcanic suites and mafic ultramafic complexes. The results of this overview should help to improve our understanding of chromitite genetic models emphasizing the significance of chromite as a powerful geotectonic indicator.

THE DATABASE

A total number of about 1400 electron microprobe analyses performed after 1990 and some bulk-ore analyses reported from Voykar Syninsky (Table 1) were initially examined. Only 1208 analyses of unaltered chromite cores and 32 bulk compositions of massive chromite containing less than 1.00 wt% SiO_2 were selected, representing 333 samples of chromitite coming from 14 different ultramafic complexes of the Urals. The compilation includes data previously published in the international literature and others taken from unpublished doctoral theses and personal data sets made available to the authors in the last two decades.

Only part of the analyses report the concentrations of NiO, MnO, V_2O_3, ZnO and Fe_2O_3. When not provided, the Fe_2O_3 content was calculated based on spinel stoichiometry. For the purpose of this work, analytical data were normalized to 100 wt%, and compositions of samples from the same locality or single drill-cores having minimal compositional variations were averaged reducing the total number of representative compositions to 52. The compositions of melts in equilibrium with chromite were calculated from 25 average chromite compositions in 14 host complexes selected according to the ore type.

GEOLOGICAL SETTING OF THE URAL CHROMITITES

The Ural orogenic belt extends over 2500 km along the 60° East Meridian (Fig. 1). It was formed by a Paleozoic continental collision subsequent to the closure of a pre-Paleozoic ocean located between the European and the Siberian-Kazakh platforms (e.g., Ivanov and Rusin, 1986). The Urals are conventionally divided into various geotectonic units, extended N-S, broadly parallel to the eastern border of the European Platform. This lateral zonation has been described by many authors (e.g., Fershtater et al., 1998) and has been schematically presented in the Proceedings of the Europrobe 1996 Project (Pérez-Estuan and Brown, 1996). A simplified scheme taken from Chashchukhin et al. (2007) is presented in Fig. 2 and includes from west to east:

i) Sedimentary and metamorphic units of the Pre-Uralian foredeep, West-Uralian zone and Central-Uralian zone extending continuosly from the Polar to the Southern Urals, east of the European continental platform. This mega-zone is limited to the east by the Main Uralian Fault (MUF) representing the westernmost and principal tectonic boundary between the collided plates.

ii) The Suture-zone and the Tagil-Magnitogorsk-zone, to the east of MUF, consist of a succession of west-verging imbricated nappes comprising fragments of oceanic lithosphere (ophiolites) and island-arc complexes, composed of plutonic and volcano-sedimentary terranes.

iii) The East-Uralian and Trans-Uralian zones are particularly developed in the south-central and Southern Urals and include transitional-oceanic to marginal and internal continental domains.

Chromitites of the Urals overviewed in this work occur associated with ophiolites and island arc plutonic complexes of the Ural-Alaskan type, distributed along the backbone of the Ural orogen (Table 2).

Chromitite in ophiolite complexes

The ophiolites are located in the Suture-zone east of MUF, (Voykar-Syninsk, Ray-Iz, Nurali) or have been obducted westward onto the European continental margin (Kraka, Kempirsai) (Fig. 2A, C). Other complexes (East-Tagil, Kluchevskoy, Alapaevskoy, Verkhneivinsky) occur as large, isolated blocks thrust over the trans-oceanic sector of the East-Uralian Zone (Fig. 2B).

The plutonic section of ophiolite sequences generally

Table 1 - Source of chromite analytical data for 333 chromitite samples from 14 selected mafic-ultramafic complexes of the Urals.

Complex	n° samples	n° analyses	References
Alapaevskoy	13	13	Chashchukhin et al. (2007).
EastTagil	2	2	Chashchukhin et al. (2007).
Kempirsai	142	203	Chashchukhin et al. (1996, 2007), Economou-Eliopoulos and Zhelyaskova-Panayotova (1998), Melcher et al. (1994), (1997), Thalhammer T.V. (1996), Ukhanov et al. (1990), Zaccarini (2005), this work.
Khabarny	21	158	Zaccarini (2005), this work.
Kluchevskoy	10	58	Chashchukhin et al. (2007), Zaccarini (2005), Zaccarini et al. (2008), this work.
Kraka	5	41	Zaccarini (2005).
Nurali	25	84	Chashchukhin et al. (1996), Grieco et al (2007), Pertsev et al. (1997), Zaccarini et al. (2004), Zaccarini (2005), Zoloev et al (2001), this work.
Ray-Iz	15	97	Ukhanov et al. (1990), Garuti et al. (1999), Zaccarini (2005).
Verkhneivinsky	3	3	Zoloev et al (2001).
Voykar Syninsky	41	41	Chashchukhin et al. (1996, 2007), Savelyev (1977).
Kachkanar	5	62	Zaccarini (2005), this work.
Kytlym	12	115	Krause et al. (2007), Zaccarini (2005), Zaccarini et al. (2011), this work.
Nizhny Tagil	20	100	Augé et a. (2005), Chashchukhin et al. (2007), Krause et al. (2007), Pushkarev and Anikina (2002), Pushkarev et al. (2007), Zaccarini (2005).
Uktus	19	170	Garuti et al. (2003), Pushkarev (2000), Zaccarini (2005).

Chromite analyses are by electron microprobe, except bulk-ore analyses from Saveliev (1977).
This work = analyses performed at the E.F. Stumpfl, EMP laboratory (University of Leoben).

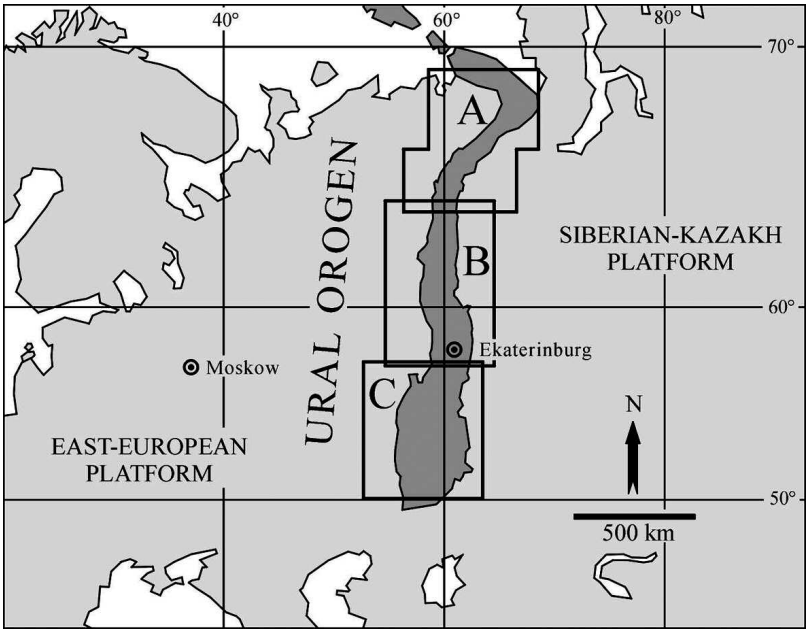

Fig. 1 - Geographic location of the Ural Orogen, marking the boundary between European and Asian continents. A) Polar and Sub-Polar Urals; B) Northern and Central Urals; C) Southern Urals. Inserts in Fig. 2.

includes residual mantle tectonite and supra-Moho layered ultramafic-mafic cumulates. Based on the geochemical characteristics of mafic and ultramafic plutonic rocks, the ophiolites appear to have been exhumed from different segments of the oceanic lithosphere. According to the criteria recently proposed by Dilek and Furnes (2011), the ophiolites of the Urals can be classified as: i) subduction-unrelated ophiolites formed in nascent spreading centers at mid oceanic ridges (MOR), back-arc basins (BA) and rifted continental margins (CM), or ii) subduction-related ophiolites evolved or emplaced in supra-subduction zones (SSZ), and volcanic arc (VA) settings.

The large ophiolite complexes of Voykar-Syninsk, Ray-Iz, Kempirsai, and Kraka contain mantle-crust sections of both the subduction-unrelated and subduction-related type, possibly indicating recession of the sub-oceanic lithosphere from the axial rifting zone towards an intra-oceanic subduction system (Saveliev and Savelieva, 1991). Subduction-unrelated mantle tectonite consists of plagioclase-lherzolite, lherzolite, and harzburgite, reflecting a low degree of partial melting (L, L-H associations). In contrast, the mantle rocks related to an intra-oceanic subduction system record a complex history of repeated partial melting and large-scale metasomatism, thereby SSZ-assemblages, which are characterized by the highly depleted harzburgite-dunite (H-D) mantle association, occur superimposed or adjacent to MOR-type assemblages of harzburgite (H), harzburgite-lehrzolite (H-L) and lherzolite (L) (Savelieva and Saveliev, 1992; Fershtater et al., 1997; 1998; Savelieva et al., 1997; Melcher et al., 1997; 1999).

The ophiolite complexes of the Polar Urals (Voykar-Syninsk and Ray-Iz) contain chromite deposits of metallurgical (high-Cr) and refractory (high-Al) grades (Fig. 3). The high-Al chromitites occur as: a) pods and elongated lenses concordant to sub-concordant with banding and lineation of the mantle tectonite, and b) true stratiform bodies concordant with the layered ultramafic rocks at the base of supra-Moho cumulate sequences (Saveliev, 1977; Perevozchikov et al., 1990, Perevozchikov and Puchkov, 1990; Savelieva, 2004). The high-Cr deposits occur mainly in the deep mantle section (Savelieva, 2004). They typically consist of podiform bodies (boudinaged lenses and veins), which may

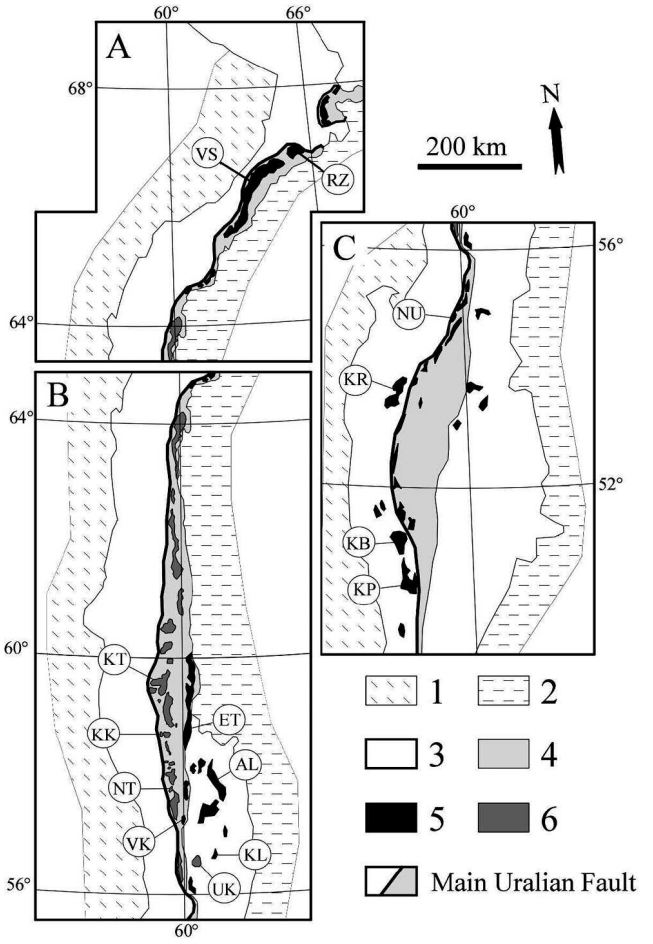

Fig. 2 - Distribution of chromitite-bearing ultramafic-mafic comlexes of the Urals overviewed in this work. A) RZ- Ray-Iz; VS- Voykar-Syninsky. B) KT- Kytlym; KK- Kachkanar; ET- East Tagil; NT- Nizhny Tagil; AL- Alapaevskoy; VK- Verkhneivinsk; KL- Kluchevskoy; UK- Uktus. C) NU- Nurali; KR- Kraka; KB- Khanarnyi; KP- Kempirsai. 1) East European Platform. 2) Siberian and Kazakhstan Platform. 3) West of the Main Uralian Fault: sedimentary and metamorphic sequences of the Pre-Uralian Foredeep, West-Uralian Zone and Central-Uralian Zone (undifferentiated); East of the Main Uralian Fault: East-Uralian and Trans-Uralian Zones (undifferentiated). 4) Suture Zone and Tagil-Magnitogorsk Mega-Zone. 5) Ophiolite complexes. 6) Concentrically-zoned Ural-Alaskan type complexes of the Platinum Bearing Belt. (Modified after Chashchukhin et al., 2007).

Table 2 - Chromitite-bearing mafic ultramafic complexes of the Urals overviewed in this work (Fig. 2).

	complex type	host rock	morphology	ore grade	Ore reserve (Mt)
Chromitite in ophiolite complexes					
Voykar-Syninsky	mantle tectonite	H-D, H	podiform	high-Cr, high-Al	>100
	supra-Moho cumulates	H	stratiform	high-Al	<10
Ray-Iz	mantle tectonite	H-D, H	podiform	high-Cr, high-Al	>100
	supra-Moho cumulates	H	stratiform	high-Al	<10
Kempirsai	mantle tectonite	H-D	podiform	high-Cr	>300
	supra-Moho cumulates	H-L	stratiform	high-Al	<10
Kraka	mantle tectonite	H-D-L	podiform	high-Cr	<10
Kluchevskoy	mantle tectonite	H-D	podiform	high-Cr	subeconomic
Alapaevskoy	?	?	?	high-Cr, high-Al	?
Verkhneivinsky	?	?	?	high-Cr, high-Al	?
East-Tagil	?	?	?	high-Cr, high-Al	?
Nurali	supra-Moho cumulates	W-PX-D	stratiform	high-Al	subeconomic
Chromitite in Ural-Alaskan-type complexes					
Kytlim	concentrically zoned	D	pods-lenses	high-Cr	<10
Kachkanar	concentrically zoned	D	veinlets	high-Cr	subeconomic
Nizhny Tagil	concentrically zoned	D	pods-lenses	high-Cr	<10
Uktus	concentrically zoned	D	veins	high-Cr	subeconomic
East Khabarny	layered intrusion	D-W	stratiform	high-Cr	<10

high-Cr = metallurgical grade, high-Al = refractory grade. H: harzburgite, L: lherzolite, D: dunite, W: websterite, PX: pyroxenite.

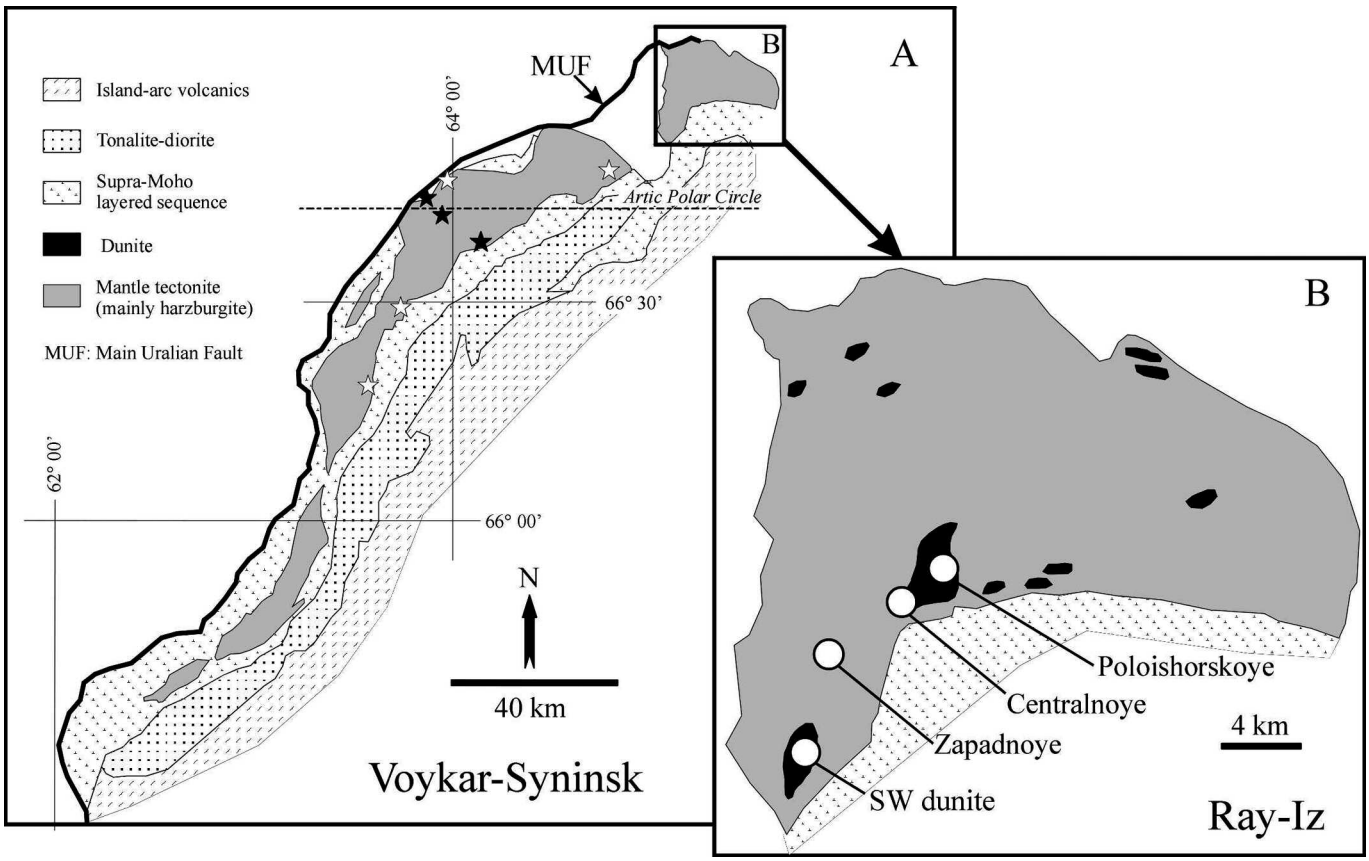

Fig. 3 - Geological sketch map of ophiolite complexes of the Polar Urals (modified after Efimov et al., 1978). A) Voykar-Syninsky, star: location of samples from Chashchukhin et al. (1996, 2007); white star = high-Al; black star = high-Cr. B) Ray-Iz, white circle: location of samples from Centralnoye drill 43, 302, 316, Zapadnoye drill 21, Poloishrskoye II outcrop (Garuti et al., 1999; Zaccarini, 2005), and SW dunite (Ukhanov et al., 1990).

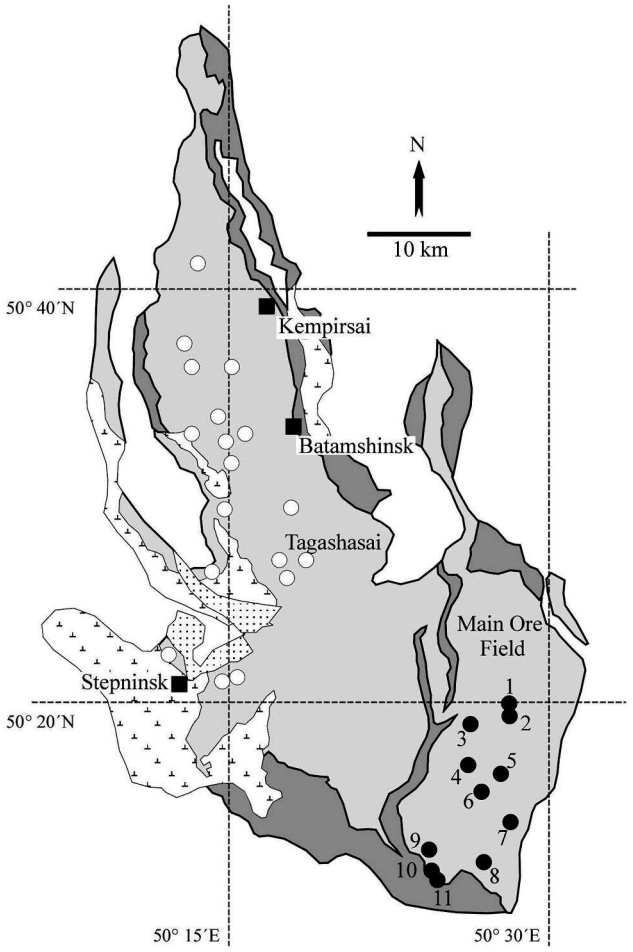

Fig. 4 - Geological sketch map of the Kempirsai ophiolite complex (modified after Savelieva et al., 1997). Sample locations: black circles = high-Cr ore deposits of the Main Ore Field; 1- 40 Years Let of Kazakh SSR; 2- Molodezhnoe; 3- drill 681; 4- Geophizicheskoe; 5- Voskhod; 6- Konsomolskoe; 7- Gigant; 8- N°21; 9- Millionnoe; 10- drill 222; 11- Diamond Pearl; open circles = high-Al deposits of the Batamshinsk, Tagashasai, and Stepninsk ore fields (Melcher et al., 1994; 1997; 1999; Chashchukhin et al., 1996; 2007; Thalhammer, 1996; Economou-Eliopoulos and Zhelyaskova-Panayotova, 1998; Zaccarini, 2005).

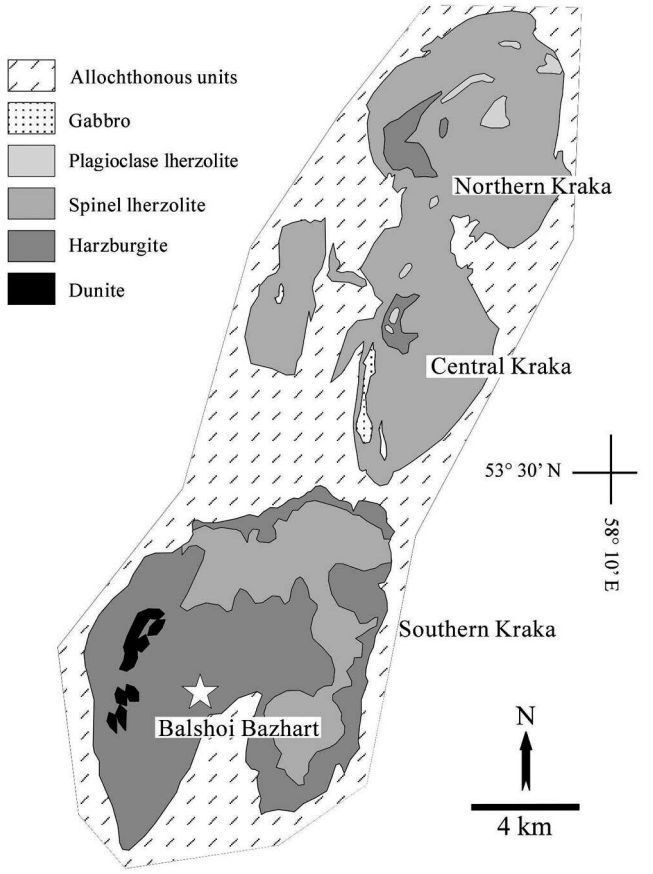

Fig. 5 - Geological sketch map of the Kraka ophiolite complex (modified after Savelieva et al., 1997). Samples studied by Zaccarini (2005) are from the Balshoi Bazhart chromium mine (open star).

extend up to more than 1 km along strike. A dunite envelope generally separates the chromitite from the harzburgite groundmass. The chromitite-dunite assemblage is less deformed than the host harzburgite, and locally exhibits low-angle intersection or clearly discordant geometric relationships with the foliation and mineral banding of the harzburgite host, indicating a late epigenetic emplacement (Pavlov and Grigoryeva, 1977; Kravchenko, 1986a; 1986b; Kravchenko and Grigoryeva, 1986; Perevozchikov et al., 1990; Perevozchikov and Puchkov, 1990).

At Kempirsai (Fig. 4), high-Cr and high-Al chromitites are found in two ophiolite blocks, separated by a major shear zone (Kravchenko and Grigoryeva, 1986; Melcher et al., 1994; 1997; 1999; Thalhammer, 1996; Savelieva et al., 1997). Typical podiform chromitites of the high-Cr type occur within subduction-related harzburgitic mantle in the SE of the complex, forming the giant chromite deposits of the Main Ore Field. Minor deposits of predominantly high-Al chromitite occur at the localities of Batamshinsk, Tagashasai and Stepninsk, in the W-NW part of the Kempirsai complex. They form concordant layers within ultramafic cumulates overlaying mantle tectonite of the subduction-unrelated type (Melcher et al., 1994; 1997; Thalhammer, 1996).

The Kraka ophiolite (Fig. 5) contains one economically significant chromite deposit of metallurgical grade (the Bolshoi Bashart mine), located in the southern mantle block where harzburgite and serpentinized harzburgite predominate over lherzolite. The other mantle blocks are characterized by spinel- and plagioclase-lherzolite subduction-unrelated assemblages and do not contain significant chromitite mineralization. The Bolshoi Bashart deposit consists of a series of boudinaged lenticular bodies up to 3-4 meters thick, which can be traced for more than 1 km along strike inside serpentinized harzburgite (Chashchukhin et al., 1996; 2002; 2007; Zaccarini, 2005).

The small ophiolite complex of Kluchevskoy is limited by major thrust faults (e.g., the Murzinsky and Kluchevskoy faults) which put the ophiolite block in tectonic contact with various units of the East-Uralian zone. The ophiolite consists of depleted mantle tectonite (harzburgite-dunite) and crustal cumulates (wherlite, clinopyroxenite, gabbro) possibly emplaced in a subduction-related setting (Fershtater et al., 1998; Zaccarini et al., 2008). The complex (Fig. 6) contains high-Cr chromitites occurring in the harzburgitic mantle

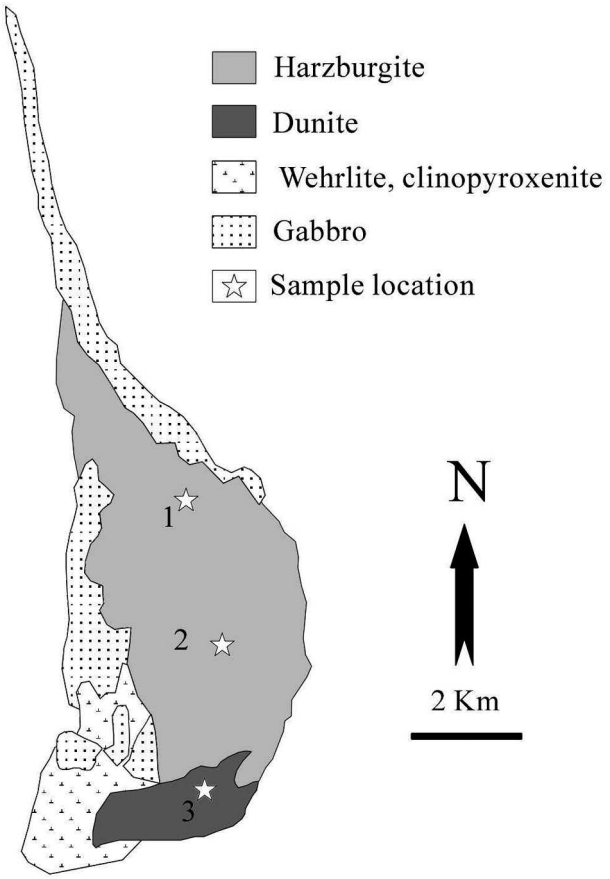

Fig. 6 - Geological sketch map of the Kluchevskoy ophiolite complex (modified after Zaccarini et al., 2008). Sample location: 1- northern harzburgite, 2- central harzburgite, 3- southern dunite trench (Chashchukhin et al., 2007; Zaccarini et al., 2008).

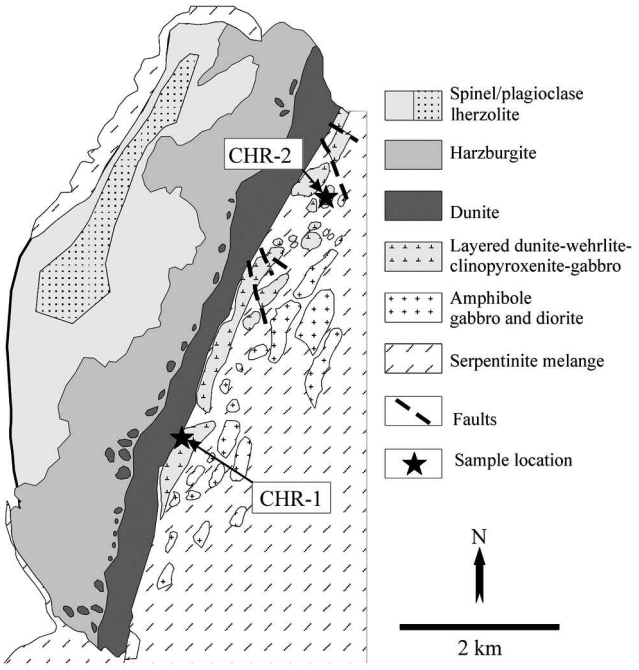

Fig. 7 - Geological sketch map of the Nurali complex and location of chromitite samples studied by Zaccarini et al. (2004).

tectonite (Chashchukhin et al., 2007) and in the dunite body, along the southern border of the harzburgite unit (Kravchenko, 1986a; 1986b; Zaccarini et al., 2008). The latter group consists of strongly folded, E-W elongated lenses of massive to disseminated chromite, dipping northwards and extending up to some hundred meters along strike. These deposits constitute the most important chromite reserve of the Kluchevskoy ophiolite (Kravchenko, 1986a).

The Nurali complex is located in the suture zone of the Southern Urals (Fig. 7). It is reported as an example of subduction-unrelated, continental-margin ophiolite (Dilek and Furnes, 2011), possibly representing lithosphere exhumed from the Asian continental margin during the early stage of collision (Fershtater et al., 1998; Zaccarini et al., 2004b; Spadea and D'Antonio, 2006). The true geological setting of the complex, however, has long been questioned by many authors, who considered the lherzolite-harzburgite-dunite sequence as a typical section through the ophiolitic mantle, resulting from progressive removal of melt in a mid-ocean ridge system (Savelieva, 1987). According to this model, the supra-Moho cumulate sequence was interpreted as a result of multiple injections of different melts derived from a progressively depleted mantle source (Petersev et al., 1997). Chromitites of a sub-economic size occur as concordant lenses at various localities within and above the transition zone (Kravchenko, 1986a; 1986b; Moloshag and Smirnov, 1996; Grieco et al., 2007). Two chromitite horizons, characterized by a high-Al composition, occur in two separated blocks of the mafic-ultramafic layered sequence, and do not show direct stratigraphic relations (Zaccarini et al., 2004b). One horizon (CHR-1) is interlayered with wehrlite-clinopyroxenite-dunite at about 150 meters above the contact with the transition-zone dunite. The other one (CHR-2) forms layers and extended lenses within a wehrlite-clinopyroxenite block isolated in the serpentinite mélange. Due to deep hydrothermal alteration, primary silicates have been largely altered into a chlorite-garnet-amphibole assemblage, with relics of chromian diopside and very rare orthopyroxene, but no fresh olivine was found (Zaccarini et al., 2004b).

The other ophiolite complexes at Alapaevskoy, Verkhneivinsky, and East-Tagil (Fig. 2B) have not been investigated in sufficient detail to be properly classified according to the criteria of Dilek and Furnes (2011). They contain both high-Cr and high-Al chromitite, however, the true nature of the host-rock association, mantle tectonite or supra-Moho cumulate sequence, is not clearly reported in the available literature.

Chromitite in Ural-Alaskan type complexes

The Alaskan type complexes of the Urals are characterized by successive crystallization of dunite, wehrlite, clinopyroxenite, gabbro, and hornblendite. They occur as: 1) pipe-like bodies with a typical concentric structure, the Ural-Alaskan type complexes *s.s.* (Fershtater and Pushkarev, 1990; Efimov et al., 1993; Ivanov, 1997; Fershtatter et al., 1999), and 2) laterally extended layered intrusions, of which the East-Khabarny complex is the best known example (Fershtater and Pushkarev, 1991; Fershtatter et al., 1997; 1998; Gottman et al., 2011). Petrography, trace element geochemistry and mineral chemistry indicate that both types of complexes crystallized from hydrous mafic melts with a high-K and calc-alkaline affinity (Fershtatter et al., 1997; 1998; 1999). Dunite typically lacks primary orthopyroxene, while all rocks contain amphibole and phlogopite. K-feldspar and

nepheline may appear in gabbros. Bulk-rock and clinopyroxene have high CaO/Al_2O_3 ratios and show negative slopes in the chondrite-normalized REE patterns, being enriched in light and middle REE up to 40 times the chondritic values (Krause et al., 2007).

The Ural-Alaskan type complexes *s.s.* overviewed in this work are exposed between the 64° and 56° north parallels (Fig. 2B). They are part of the so-called "Urals Platinum Belt" (UPB), which houses the historically known load and placer Pt-deposits of the Urals (Duparc and Tikonowitch, 1920; Razin, 1976; Efimov and Tavrin, 1978; Efimov et al., 1993; Ivanov, 1997; Fershtatter et al., 1999; Pushkarev and Anikina, 2002; Garuti et al., 2002; 2003; Johan, 2002). The concentrically zoned pipes seem to intrude, or are tectonically emplaced, into the gabbro-diorite formation of the Silurian Tagil island-arc (Kytlym, Nizhny Tagil, and Kachkanar). In one case (Uktus), the complex appears to be emplaced out of this zone in a continental margin setting (Fig. 2B). In contrast, the East-Khabarny layered intrusion is part of the allochthonous Khabarny ophiolite complex (Southern Urals, Fig. 2C), possibly having intrusive relations with residual mantle harzburgite in a sub-oceanic lithosphere.

In the concentrically zoned pipes, chromitite occurs exclusively in the dunite member and is generally of the high-Cr type. Betekhtin (1961) classified the chromitites into two structural types, "syngenetic" and "epigenetic", suggestive of two stages of chromite precipitation with respect to the host dunite.

Syngenetic chromitites display textural and chemical equilibrium with the dunite host suggesting crystallization at a high temperature (Garuti et al., 2003). They are common in all complexes usually in the form of wispy vermiculations to decimeter-size veinlets, schlieren and irregular pods. Thin lenses and layers up to some meters long are rare, apparently restricted to the Kytlym complex (Fig. 8A), the Solovyeva quarry of Nizhny Tagil (Fig. 8B), and the southern dunite body of Uktus (Fig. 8D) (Pushkarev, 2000; Garuti et al., 2003; Augé et al., 2005; Zaccarini, 2005; Chashchukhin et al., 2007; Zaccarini et al., 2011). Some samples from Uktus display textural evidence of metamorphic re-crystallization (Chashchukhin et al., 2007).

Epigenetic chromitites have been reported from the complexes of Nizhny Tagil and Kytlym. The most common type consists of centimeters-thick, waving veins infiltrating the

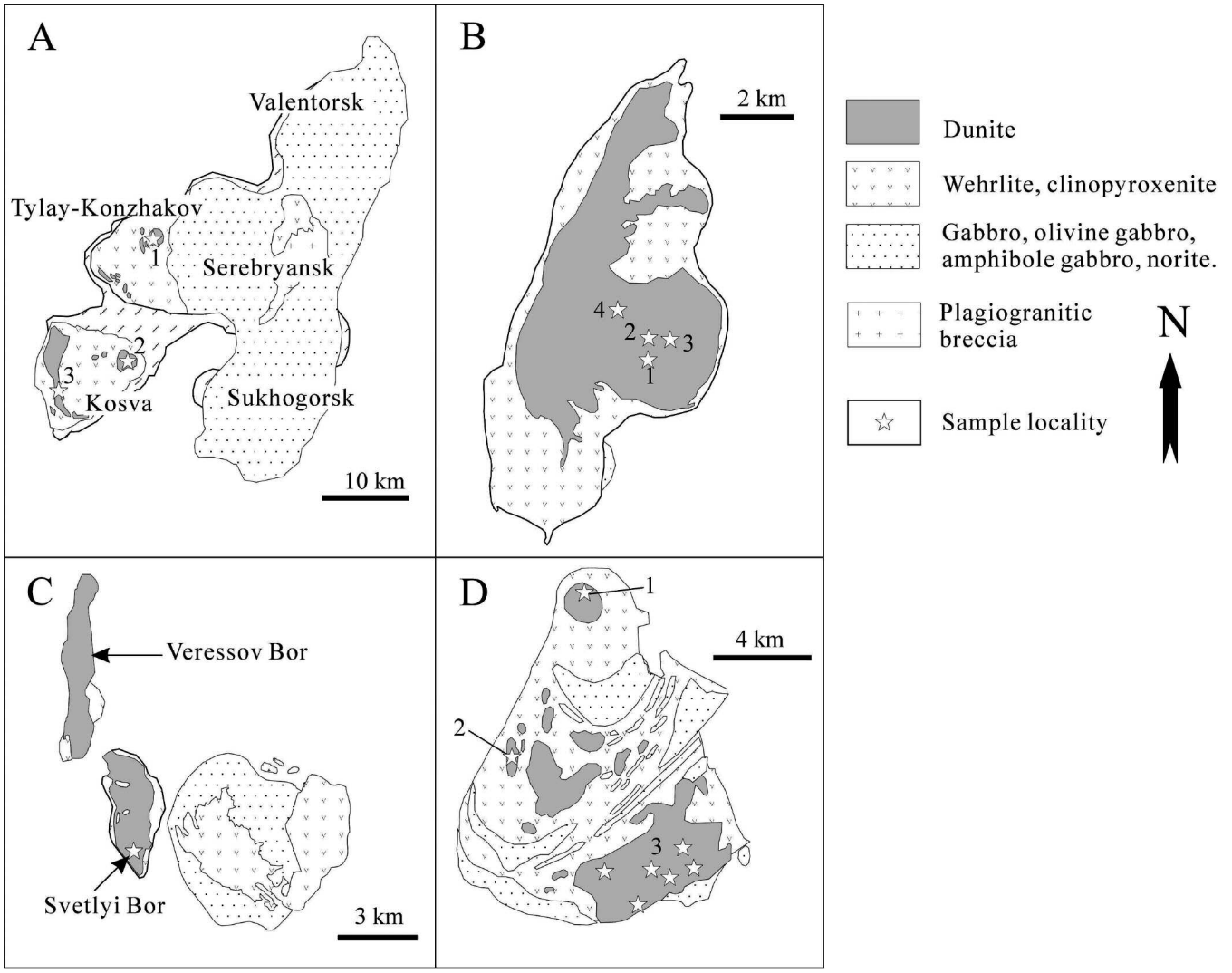

Fig. 8 - Geological sketch maps of selected Ural-Alaskan intrusions of the Urals. A) Kytlym, sample location: 1- Tylay-Konzhakov; 2- Kosva East; 3- Kosva W. B) Nizhny Tagil: 1- Solovyeva quarry; 2- Alexandrovsky; 3- Sirkov log; 4- Gosshkhta. C) Kachkanar: 1- sample location at Svetily Bor. D) Uktus. 1- northern dunite; 2- western dunite; 3- southern dunite (Pushkarev, 2000; Pushkarev and Anikina, 2002; Garuti et al., 2003; Augé et al., 2005; Chashchukhin et al., 2007; Krause et al., 2007; Pushkarev et al., 2007).

massive dunite. The veins may be arranged in dendritic or anastomosing patterns, including patches of strongly serpentinized dunite. At Nizhny Tagil, chromitite may form the cement of a dunite breccia consisting of angular or smoothly eroded fragments up to several centimeters in size (Betekhtin, 1961; Puskarev and Anikina, 2002; Pushkarev et al., 2007). In all these cases, a millimeter-thick rim of serpentine develops at the contact between chromitite and the host dunite (Puskarev and Anikina, 2002). A special type of epigenetic chromitite occurs in the "Butyrin vein" cutting across dunite in the Kytlym complex (Zaccarini et al., 2011, and references therein). The vein is generally a few centimeters in thickness, and is predominately composed of amphibole-rich clinopyroxenite with accessory orthopyroxene, olivine, and an internal zone enriched in disseminated and massive chromite. The contact between the mineralized vein and the host dunite is sharp and is marked by a 0.5- to 3-mm-thick rim of orthopyroxene.

The East Khabarny layered complex contains potential chromite deposits located in the basal zone of a kilometer-thick dunite horizon passing upwards into clinopyroxenite, websterite and gabbro-norite (Fig. 9). The ore bodies consist of zones of chromitite-dunite layering up to several meters thick, dipping 30-40° westwards, concordant with lithological boundaries. Chromitite forms centimeters-thick, massive layers or lenses of intensive chromite dissemination extending several tens of meters along strike (Kravchenko, 1986a; 1986b; Zaccarini, 2005).

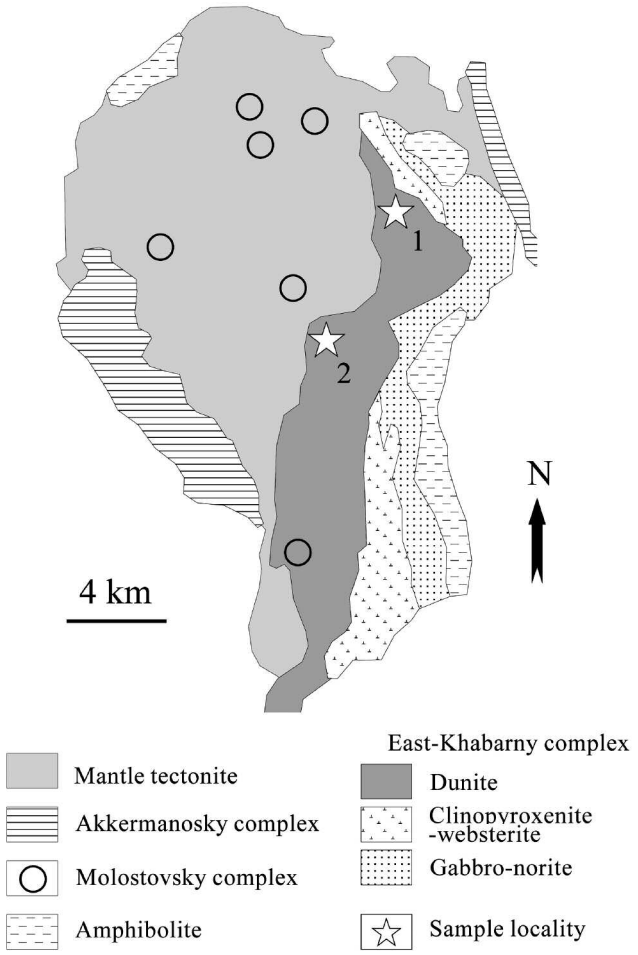

Fig. 9 - Geological sketch map of the Khabarny complex (modified after Gottman et al., 2011). Mantle tectonite: predominant harzburgite with subordinate lherzolite. East- Khabarny layered sequence: amphibole- and phlogopite-bearing dunite, clinopyroxenite, websterite, gabbro-norite and hornblendite with Ural-Alaskan magmatic affinity (Fershtater and Pushkarev 1991, Fershtatter et al. 1997, 1998, Gottman et al. 2011). Chromitite samples studied by Zaccarini (2005) are located close to the base of the dunite unit, Star 1: quarry 5/2, Star 2: top of the hill. Open circle: location of ultramafic-alkaline intrusions of the Molostovsky complex. Akkermanosky complex: ophiolitic supra-Moho cumulates (dunite, wehrlite, clinopyroxenite, gabbro-norite, plagiogranite), overlain by sheeted-dike complex and bononitic lavas.

CHROMITE MINERAL CHEMISTRY

Average electron microprobe compositions of chromite from chromitites of the Urals (Table 3) define distinctive fields on the Cr# [= Cr/(Cr + Al)] vs. Mg# [= Mg/(Fe^{2+} + Mg)] diagram, according to the type of host complex and the geometry of the ore bodies: podiform chromitite in ophiolitic mantle, stratiform chromitite in ophiolitic supra-Moho cumulates, and podiform to stratiform chromitite in Ural-Alaskan type complexes.

Podiform chromitites hosted in ophiolitic mantle (Fig. 10A) are characterized by a narrow range in Mg# (0.52-0.83) and a wide range in Cr# (0.35-0.87). The chromites of metallurgical grade (high-Cr) have Cr# > 0.70, whereas those of refractory grade (high-Al) are characterized by Cr# < 0.70. The general trend of increasing Cr# broadly reflects the increase of the degree of partial melting of the mantle source of the chromitite parental melts (Dick and Bullen, 1984; Arai, 1992; 1997; Roeder, 1994; Barnes and Roeder, 2001). However, some samples from the Voykar-Syninsky complex define trends of Fe^{2+} enrichment (low Mg#) typical of metamorphic spinels (Evans and Frost, 1975).

The stratiform chromitites from supra-Moho cumulate sequences vary greatly in Cr# and Mg# (Fig. 10B). One group (Kempirsai, Ray-Iz, Voykar-Syninsky, Nurali CHR-1) has high Mg# (> 0.50) and low Cr# (< 0.51). A second group containing the chromitite from Nurali CHR-2 is enriched in iron with respect to group 1 (Mg# < 0.50) and has slightly higher Cr# (> 0.50) compared with CHR-1 (Cr# < 0.51).

The Ural-Alaskan trend, including chromitites from the East-Khabarny complex, is characterized by a decrease of Mg# with decreasing Cr# (Fig. 10C), which is typical of stratiform chromitites of the Bushveld type, apparently reflecting magmatic differentiation. A wide range of differentiation is seen in syngenetic chromitites from the north and south dunite bodies of the Uktus complex (Garuti et al., 2003). The differentiation trend involves a progressive enrichment in total iron and depletion in Mg and Cr, parallel to a decrease of FeO/MgO in bulk dunite and olivine. Epigenetic chromitite veins from Nizhny Tagil show a symmetrical zoning with a decrease in Cr_2O_3 and MgO, and an increase in total FeO from the core to the rims of the ore bodies (Pushkarev and Anikina, 2002; Pushkarev et al., 2007). Epigenetic chromite from the Butyrin vein has the lowest Mg# due to the exceptional enrichment in total Fe, although no core-rim zoning was observed across the chromitite veins (Zaccarini et al., 2011). The whole Cr#-Mg# covariation trend in epigenetic chromitite displays positive correlation similar to the syngenetic type. However, the Cr# variation is comparatively narrow compared to a wide range in Mg# (Pushkarev and Anikina, 2002; Pushkarev et al., 2007).

Table 3a - Average compositions of chromite from podiform chromitites hosted by ophiolitic mantle rocks of the Urals.

host complex	locality/mine	n°	ore type	TiO_2	Al_2O_3	FeO	Fe_2O_3	MgO	MnO	Cr_2O_3	NiO	ZnO	V_2O_3	Fe^{2+}#	Cr#	Fe^{3+}#
Voykar Syninsky		14	Cr-rich	0.26	9.91	13.16	5.97	12.08	0.09	58.53	0.00	0.00	0.00	0.38	0.80	0.07
Voykar Syninsky		21	Al-rich	0.23	27.19	11.53	5.46	16.53	0.09	38.97	0.00	0.00	0.00	0.29	0.49	0.06
Ray-Iz	Zapadnoye	2	Cr-rich	0.11	10.26	12.74	4.74	13.44	0.24	58.15	0.10	0.10	0.10	0.35	0.79	0.06
Ray-Iz	Centralnoye	3	Cr-rich	0.13	10.39	11.36	4.03	14.34	0.26	59.12	0.12	0.15	0.11	0.31	0.79	0.05
Ray-Iz	Poloishorkoye II	3	Cr-rich	0.08	8.62	12.83	4.65	13.20	0.28	60.03	0.11	0.11	0.10	0.35	0.82	0.06
Ray-Iz	SW dunite	2	Al-rich	0.19	15.93	12.54	4.26	14.32	0.19	52.47	0.10	0.00	0.00	0.33	0.69	0.05
Kempirsai	40 Years Kazakh SSR	17	Cr-rich	0.11	9.05	9.56	4.93	15.53	0.22	60.55	0.05	0.00	0.00	0.26	0.82	0.06
Kempirsai	Mololodezhnoe	9	Cr-rich	0.12	9.39	10.10	4.24	15.17	0.10	60.65	0.17	0.02	0.05	0.27	0.81	0.05
Kempirsai	drill 681	13	Cr-rich	0.21	9.98	14.26	4.15	12.41	0.41	58.46	0.11	0.00	0.00	0.39	0.80	0.05
Kempirsai	Geophizicheskoe	3	Cr-rich	0.31	8.75	12.18	4.48	13.79	0.25	60.03	0.09	0.09	0.04	0.33	0.82	0.05
Kempirsai	Voskhod	5	Cr-rich	0.13	8.95	10.14	4.60	15.37	0.27	60.39	0.11	0.04	0.00	0.27	0.82	0.06
Kempirsai	Kornsomol'skoe	1	Cr-rich	0.02	8.66	8.27	5.09	16.19	0.34	61.33	0.09	0.00	0.00	0.22	0.83	0.06
Kempirsai	Gigant	1	Cr-rich	0.02	9.50	9.37	4.46	15.55	0.33	60.65	0.13	0.00	0.00	0.25	0.81	0.05
Kempirsai	N°21	1	Cr-rich	0.02	8.96	10.66	2.39	14.75	0.29	62.85	0.04	0.04	0.00	0.29	0.82	0.03
Kempirsai	Millionnoe	1	Cr-rich	0.02	9.64	9.88	3.59	15.27	0.28	61.18	0.15	0.00	0.00	0.27	0.81	0.04
Kempirsai	drill 222	11	Cr-rich	0.18	9.24	10.79	2.78	14.58	0.38	61.87	0.18	0.00	0.00	0.29	0.82	0.03
Kempirsai	Diamond Pearl	16	Cr-rich	0.09	9.56	10.77	4.03	14.83	0.30	60.36	0.05	0.02	0.00	0.29	0.81	0.05
Kempirsai	MOF*	22	Cr-rich	0.17	10.07	11.80	3.72	14.11	0.34	59.76	0.01	0.01	0.01	0.32	0.80	0.05
Kraka	Bolshoi Bashart	5	Cr-rich	0.17	12.84	11.63	4.65	14.53	0.21	55.77	0.08	0.06	0.05	0.31	0.74	0.06
Kluchevskoy	N-Hz	1	Cr-rich	0.10	12.42	12.51	2.36	14.10	0.00	58.50	0.00	0.00	0.00	0.33	0.76	0.03
Kluchevskoy	central-Hz	3	Cr-rich	0.27	11.17	14.51	7.14	12.50	0.33	54.08	0.00	0.00	0.00	0.39	0.76	0.09
Kluchevskoy	S-dunite	6	Cr-rich	0.19	11.64	14.78	4.65	12.25	0.32	55.89	0.09	0.08	0.11	0.40	0.76	0.06
Verkhneivinsky		2	Al-rich	0.15	17.59	12.34	2.63	14.60	0.26	52.43	0.00	0.00	0.00	0.32	0.67	0.03
Verkhneivinsky		1	Cr-rich	0.14	8.66	16.34	0.00	10.99	0.33	63.55	0.00	0.00	0.00	0.45	0.83	0.00
EastTagil		2	Al-rich	0.24	22.36	12.02	1.79	15.35	0.29	47.96	0.00	0.00	0.00	0.31	0.59	0.02
Alapaevskoy		1	Cr-rich	0.32	10.15	12.19	4.73	13.98	0.31	58.32	0.00	0.00	0.00	0.33	0.79	0.06
Alapaevskoy		12	Al-rich	0.26	23.78	12.60	3.95	15.13	0.25	44.03	0.00	0.00	0.00	0.32	0.55	0.05

n° = number of averaged samples (total 178). MOF*: undefined locality in the Main Ore Field.

Table 3b - Average compositions of chromite from stratiform chromitites in supra-Moho ophiolitic cumulates of the Urals.

host complex	locality/mine	n°	ore type	TiO2	Al2O3	FeO	Fe2O3	MgO	MnO	Cr2O3	NiO	ZnO	V2O3	Fe2#	Cr#	Fe3#
Voykar Syninsky		6	Al-rich	0.38	22.20	17.86	4.87	11.56	0.26	42.72	0.03	0.00	0.12	0.47	0.57	0.06
Kempirsai	NWF*	8	Al-rich	0.20	26.22	13.63	2.66	14.68	0.20	42.26	0.15	0.00	0.00	0.34	0.52	0.03
Kempirsai	Stepninsk	5	Al-rich	0.08	27.33	15.35	4.97	13.44	0.32	38.28	0.14	0.08	0.00	0.40	0.49	0.06
Kempirsai	Batamshinskoe	11	Al-rich	0.12	26.18	11.95	3.29	15.54	0.21	42.48	0.15	0.04	0.03	0.30	0.52	0.04
Kempirsai	Tagashasai	18	Al-rich	0.22	28.08	15.65	6.30	13.44	0.26	35.92	0.13	0.00	0.00	0.40	0.46	0.07
Ray-Iz	Al-rich	5	Al-rich	0.14	25.40	15.29	3.35	13.02	0.15	42.54	0.10	0.00	0.00	0.40	0.53	0.04
Nurali	CHR-1	7	Al-rich	0.08	28.71	13.73	5.33	14.75	0.19	36.90	0.15	0.05	0.10	0.35	0.46	0.06
Nurali	CHR-2	4	Al-rich	0.77	19.75	21.08	15.17	9.26	0.32	33.25	0.13	0.11	0.16	0.56	0.53	0.19
Nurali		2	Cr-rich	0.17	8.91	12.98	4.24	13.33	0.20	60.18	0.00	0.00	0.00	0.35	0.82	0.05
Nurali		10	Al-rich	0.39	16.52	17.19	7.60	11.38	0.34	46.58	0.00	0.00	0.00	0.46	0.65	0.09
Nurali		2	Al-rich	0.05	28.90	10.82	5.57	16.64	0.25	37.76	0.00	0.00	0.00	0.27	0.47	0.06

n° = number of averaged samples (total 78). NWF*: undefined locality in the NW ore field.

Table 3c - Average compositions of chromite from chromitites in Alaskan-type complexes of the Urals.

host complex	locality/mine	n°	ore type	TiO2	Al2O3	FeO	Fe2O3	MgO	MnO	Cr2O3	NiO	ZnO	V2O3	Fe2#	Cr#	Fe3#
Kytlym	Tylay-Konzhakov I	3	syngentic	0.67	9.93	17.78	16.71	10.27	0.33	44.01	0.13	0.07	0.09	0.50	0.75	0.22
Kytlym	Kosva (E dunite)	5	syngentic	0.84	10.17	16.95	19.24	10.96	0.31	41.24	0.10	0.09	0.10	0.46	0.73	0.25
Kytlym	Kosva (W dunite)	1	syngentic	0.50	4.62	24.06	40.66	5.19	0.61	24.36	0.00	0.00	0.00	0.72	0.78	0.55
Nizhny Tagil	Solovyeva	10	syngentic	0.42	7.69	16.27	14.03	10.90	0.42	50.15	0.06	0.05	0.02	0.46	0.81	0.18
Nizhny Tagil	Alexandrovsky	2	syngentic	0.34	7.12	16.39	11.92	10.33	0.48	53.23	0.03	0.13	0.03	0.48	0.83	0.14
Nizhny Tagil	Sirkov log	3	syngentic	0.35	7.99	14.13	9.86	12.42	0.34	54.68	0.15	0.09	0.00	0.40	0.82	0.13
Kachkanar	Svetily Bor	5	syngentic	0.50	7.64	16.56	13.33	10.75	0.40	50.62	0.10	0.06	0.03	0.47	0.82	0.17
Uktus	N-dunite	7	syngentic	1.00	11.66	19.41	17.22	9.40	0.38	40.55	0.11	0.07	0.19	0.54	0.69	0.22
Uktus	W-dunite	2	syngentic	0.55	11.45	18.28	8.41	10.11	0.50	50.70	0.00	0.00	0.00	0.50	0.75	0.11
Uktus	S-dunite	10	syngentic	0.61	12.92	15.77	9.73	12.03	0.31	48.31	0.13	0.09	0.11	0.42	0.72	0.12
Nizhny Tagil	Gosshkhta	5	epigenetic	0.47	7.11	15.96	15.59	11.06	0.48	49.32	0.00	0.00	0.00	0.45	0.82	0.20
Kytlym	Butyrin vein	3	epigenetic	2.98	5.17	28.42	33.73	4.07	0.50	25.05	0.02	0.02	0.04	0.80	0.77	0.50
Khabarny	quarry 5/2	8	stratiform	0.47	11.33	13.91	7.96	13.14	0.32	52.78	0.04	0.02	0.03	0.37	0.76	0.10
Khabarny	top of the hill	13	stratiform	0.82	9.52	20.12	11.74	8.84	0.44	48.27	0.08	0.06	0.09	0.56	0.77	0.15

n° = number of averaged samples (total 77).

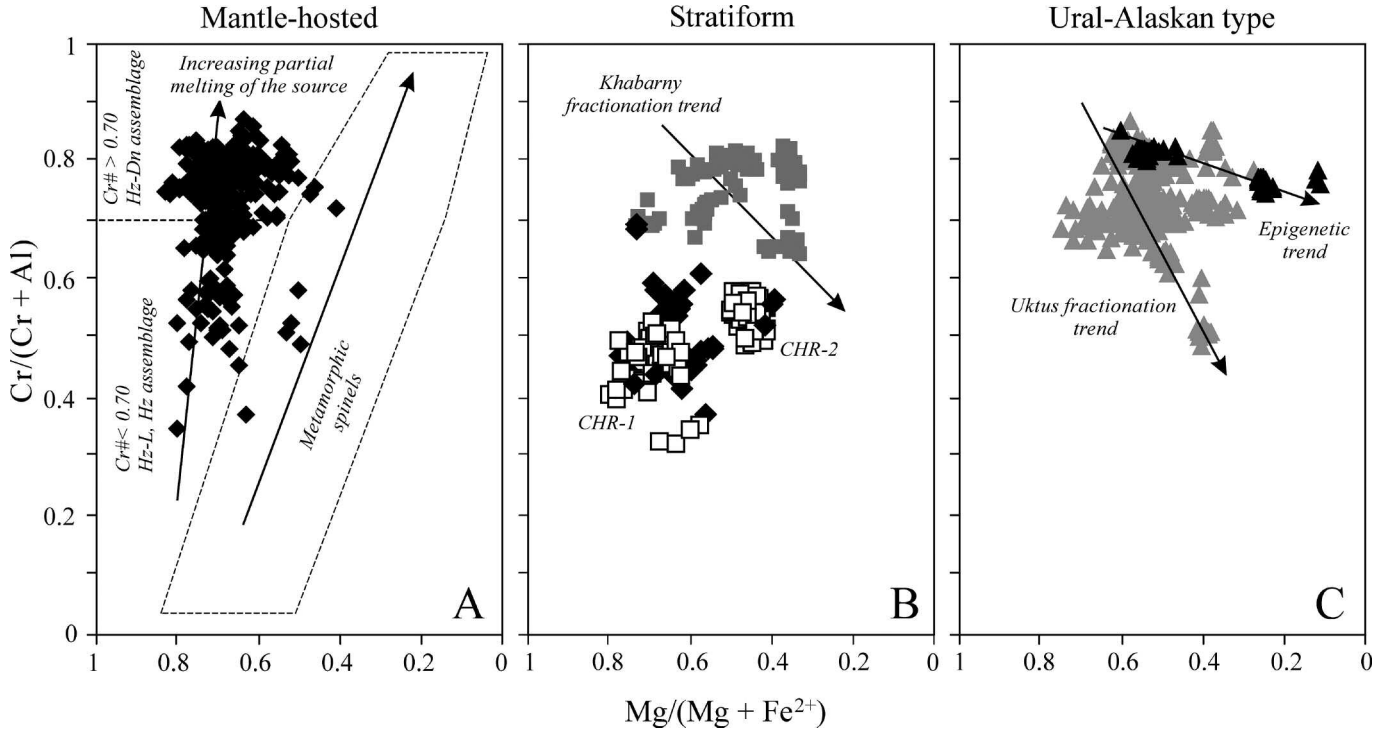

Fig. 10 - Plot of the 1240 chromite analyses database on the Cr# [= Cr/(Cr+Al)] vs. Mg# [= Mg/(Fe^{2+}+Mg)] diagram. A) Podiform chromitites hosted by the mantle units of ophiolite complexes. Some samples from Voykar Syninsky show a Fe^{2+} enrichment typical of metamorphic spinels (Evens and Frost 1975). B) Stratiform chromitites in supra-Moho cumulate sequences of the Kempirsai, Voykar Syninsky and Ray-Iz ophiolite complexes (black diamond), Nurali (open square), and stratiform chromitites in the dunite unit of the East-Khabarny layered complex (grey square). The CHR-1 and CHR-2 chromitite layers of Nurali clearly display different Mg#. Compositions from East-Khabarny overlap the field of Ural-Alaskan type chromitite. C) Syngenetic (grey triangle) and epigenetic (black triangle) chromitites in Alaskan-type concentrically zoned complexes of the Urals. Note the different fractionation trends of the syngenetic and epigenetic chromitites (Pushkarev et al., 2007).

The TiO_2 content of chromite displays significant variations (Table 3). With the exception of some high-Al samples, the TiO_2 content is usually lower than 0.30 wt% in podiform chromitites from ophiolitic mantle, and in the Fe-poor supra-Moho stratiform chromitites (Fig. 11A, B). The Fe-rich stratiform chromitites of Nurali CHR-2 have high TiO_2 contents falling in the range of 0.50-0.90 (Fig. 11B). In chromitites of the East-Khabarny (Fig. 11B) and Ural-Alaskan type complexes (Fig. 11C), the TiO_2 content increases from 0.37 to 1.30 wt% as a result of differentiation, but can be as high as 2.3-3.5 wt% in the Butyrin veins of Kytlym (Fig. 11C). Variations of Fe^{3+}# [= Fe^{3+}/(Cr + Al + Fe^{3+})] with Mg# mimics the TiO_2 trend, indicating a general increase of Fe^{3+} with differentiation (Fig. 11D, E, F). The Ural chromitites show contrasting trends of substitution in the Cr-Al-Fe^{3+} triangle. Mantle-hosted chromitites (Fig. 12A) show a wide Cr-Al exchange at relatively low Fe^{3+}, in contrast with Ural-Alaskan chromitites, which are dominated by a Cr-Fe^{3+} substitution trend (Fig. 12C). The amount of Fe^{3+} may exceed the miscibility gap for natural spinels (Roeder, 1984). This leads to chromite grains exhibiting spectacular lamellar exsolution between chromian magnetite and picotite with accessory geikielite (Pushkarev et al., 1999; Garuti et al., 2003; Krause et al., 2011). The stratiform chromitites display a two-fold trend of trivalent metal substitution. The group characterized by a Fe-poor composition (Kempirsai, Ray-Iz, Nurali CHR-1) overlaps the trends of ophiolitic chromitites. In contrast, the Fe-rich chromite from Nurali CHR-2 has a distinctly high Fe^{3+}content, and compositions from East-Khabarny overlap the trend of Ural-Alaskan chromitites (Fig. 12B).

CHROMITE-OLIVINE PHASE RELATIONS AND OXYGEN THERMO-BAROMETRY

Olivine composition

Olivine is a common accessory mineral in most chromitites of the Urals, except for Nurali, where Cr-diopside seems to be the only silicate preserved by alteration (Zaccarini et al., 2004b). In general, olivine occurs as small inclusions (up to ~ 200 μm) engulfed in unaltered chromite grains, or as large grains interstitial to massive chromite. Olivine displays a wide range of magnesium number (Mg#) with distinctive Ni, Mn and Ca contents according to the type of the host chromitite (Table 4). Most of the olivine from ophiolitic mantle chromitites (Kempirsai, Ray-Iz, Kraka, Kluchevskoy) has high forsterite contents (Fo = 94-98%) and NiO concentrations (0.35-1.15 wt%), with low MnO (< 0.15 wt%), and CaO usually below the EMP detection limit (Fig. 13). Exceptionally low Fo% down to 90 are reported by Chashchukhin et al. (1996; 2007) for chromitites from Kempirsai, Voykar Syninsky and Alapaevskoy (not shown in Fig. 13). Olivine from cumulus chromitites is moderately forsteritic (Fo = 90-93%) and NiO poor (0.31-0.48 wt%), with MnO and CaO contents in the same range as in olivine from ophiolitic mantle chromitites (Fig. 13). Olivines in chromitites from East Khabarny and Ural-Alaskan intrusions show a wide range of forsterite contents (Fo = 82-99%) at NiO contents below 0.50 wt%. They have exceptionally high MnO and CaO contents up to 0.45 wt% and 0.50 wt%, respectively (Zaccarini, 2005). Manganese shows a negative correlation with the forsterite content possibly reflecting fractional crystallization (Fig. 13). Systematic

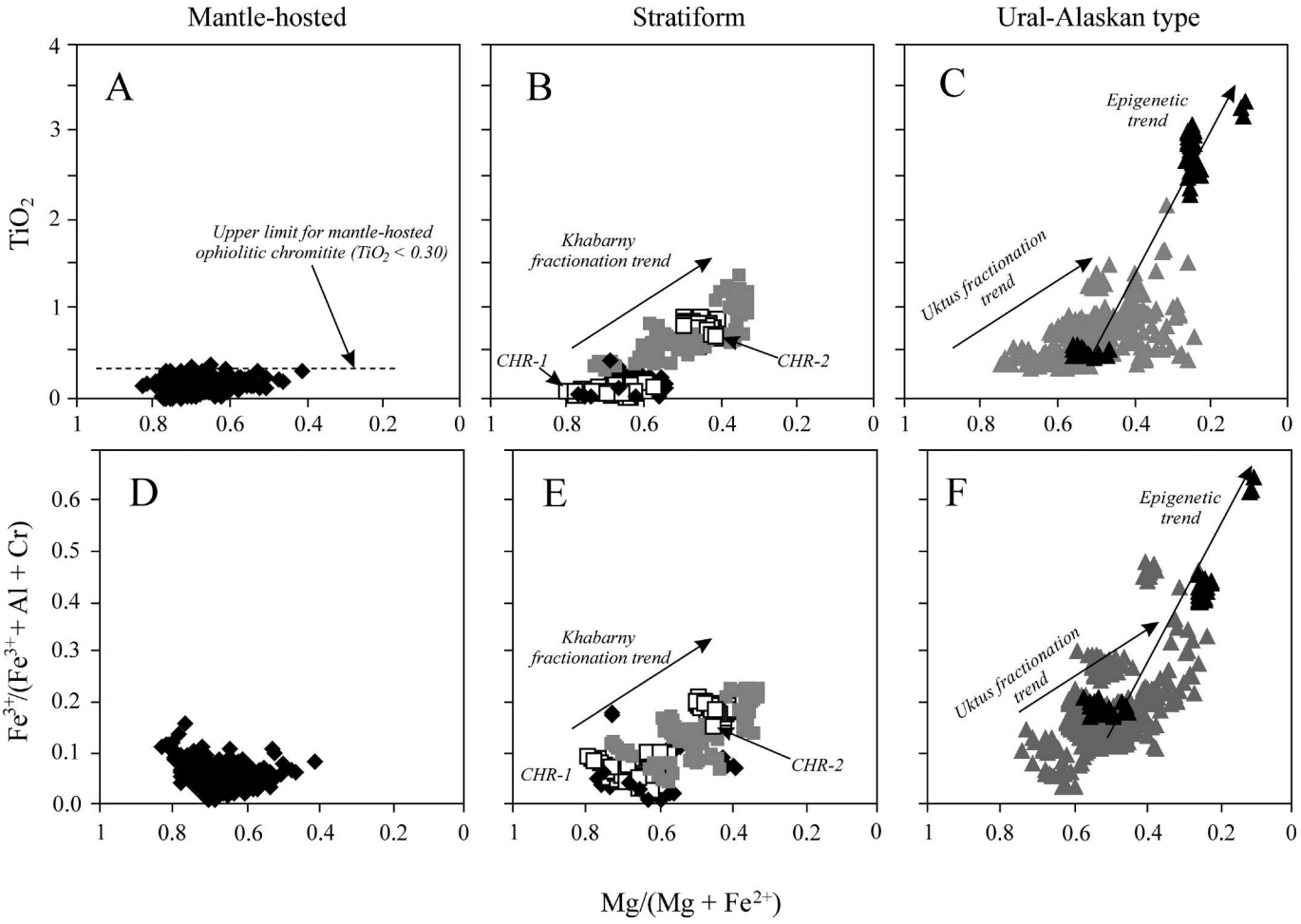

Fig. 11 - Variation of TiO_2 and Fe^{3+}# [= Fe^{3+}/(Cr+Al+ Fe^{3+})] as functions of Mg# [= Mg/(Fe^{2+}+Mg)] for 1240 chromite analyses. A-D) Podiform chromitites hosted by the mantle tectonite unit of ophiolite complexes. B-E) Stratiform chromitites in supra-Moho cumulate sequences of the Kempirsai, Voykar Syninsky and Ray-Iz ophiolite complexes, Nurali, and stratiform chromitites in the dunite unit of the East-Khabarny layered complex. C-F) Syngenetic and epigenetic chromitites in concentrically zoned complexes of the Urals (Ural-Alaskan type). (Symbols as in Fig. 10). Note the exceptionally high TiO_2 and Fe^{3+} contents in the epigenetic chromitites of the concentrically zoned complexes of the Urals.

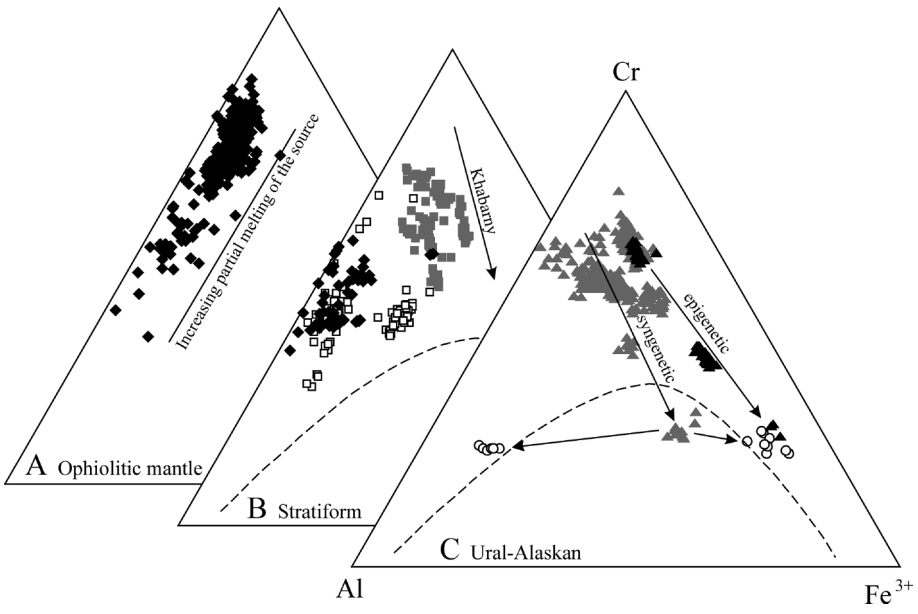

Fig. 12 - Ternary Al-Cr-Fe^{3+} plot for the 1240 chromite analyses database. A) Podiform chromitites hosted by the mantle tectonite unit of ophiolite complexes. B) Stratiform chromitites in supra-Moho cumulate sequences of the Kempirsai, Voykar Syninsky and Ray-Iz ophiolite complexes, Nurali, and stratiform chromitites in the dunite unit of the East-Khabarny layered complex. C) Syngenetic and epigenetic chromitites in concentrically zoned complexes of the Urals (Ural-Alaskan type). The dashed line in B and C represents the approximate position of the miscibility gap for natural spinels (Roeder, 1994). Note that chromitites in the northern dunite of Uktus showing unmixing-texture into "picotite" and "chromian-titanomagnetite" (Fig. C, open circles) has a Fe-rich bulk composition (measured by Garuti et al., 2003) within the "spinel miscibility gap". (Other symbols as in Fig. 10).

Table 4 - Selected Electron microprobe composition of accessory olivine in chromitites of the Urals.

Host complex	locality/mine	SiO_2	TiO_2	Al_2O_3	FeO	MgO	MnO	CaO	Na_2O	K_2O	Cr_2O_3	NiO	ZnO	V_2O_3	Tot	#Mg
Kempirsai	Diamond Pearl	42.50	0.05	0.03	2.05	52.98	0.00	0.00	0.00	0.00	1.25	1.00	0.00	0.00	99.86	0.979
Kempirsai	40 Years Kazakh SSR	42.49	0.05	0.00	2.34	53.53	0.02	0.00	0.00	0.00	0.80	1.08	0.00	0.00	100.31	0.976
Kempirsai	Voskhod ?	42.32	0.03	0.00	3.69	53.12	0.07	0.00	0.00	0.00	0.75	0.64	0.00	0.00	100.62	0.962
Kempirsai	Batamshinskoe	41.40	0.00	0.00	4.62	53.70	0.06	0.00	0.00	0.00	0.60	0.52	0.00	0.00	100.90	0.954
Kluchevskoy	S-dunite	43.07	0.00	0.04	4.10	51.64	0.04	0.03	0.02	0.00	0.00	0.34	0.00	0.01	99.29	0.957
Kluchevskoy	S-dunite	43.67	0.02	0.02	3.26	52.02	0.00	0.07	0.04	0.01	0.00	0.40	0.00	0.02	99.54	0.966
Kluchevskoy*	S-dunite	42.10	0.00	0.07	2.38	53.71	0.09	0.03	0.00	0.00	1.02	0.47	0.01	0.02	99.90	0.976
Kluchevskoy*	S-dunite	42.59	0.00	0.07	2.32	53.24	0.09	0.03	0.00	0.00	0.99	0.46	0.01	0.02	99.82	0.976
Kraka	Bolshoi Bashart	41.22	0.02	0.02	7.03	50.41	0.09	0.06	0.18	0.00	0.01	0.26	0.07	0.00	99.37	0.927
Kraka	Bolshoi Bashart	41.18	0.01	0.00	6.89	51.06	0.07	0.05	0.01	0.00	0.00	0.33	0.09	0.00	99.70	0.930
Ray-Iz	Centralnoye	42.47	0.00	0.00	3.18	53.06	0.09	0.00	0.00	0.00	0.03	0.71	0.20	0.00	99.74	0.967
Ray-Iz *	Centralnoye	41.33	0.00	0.00	2.54	54.75	0.03	0.00	0.00	0.00	0.22	0.70	0.13	0.00	99.69	0.977
Ray-Iz	Poloishorkoye II	42.29	0.03	0.00	3.14	53.55	0.11	0.00	0.00	0.00	0.04	0.60	0.15	0.02	99.92	0.968
Ray-Iz*	Poloishorkoye II	47.08	0.03	0.00	2.30	48.30	0.02	0.00	0.00	0.00	1.03	0.76	0.00	0.00	99.52	0.974
Khabarny	quarry 5/2	41.15	0.01	0.04	8.86	48.78	0.00	0.10	0.04	0.01	0.04	0.13	0.00	0.01	99.16	0.907
Khabarny	top of the hill	40.66	0.03	0.03	10.50	48.72	0.23	0.10	0.10	0.00	0.03	0.40	0.00	0.02	100.82	0.892
Khabarny	top of the hill	38.99	0.00	0.01	14.42	46.82	0.24	0.08	0.03	0.00	0.00	0.16	0.00	0.00	100.75	0.853
Kytlym	Konzhakov	42.45	0.07	0.18	3.08	54.41	0.03	0.02	0.13	0.00	0.31	0.21	0.00	0.00	100.89	0.969
Kytlym	Kosva	43.74	0.01	0.00	5.97	48.74	0.02	0.24	0.03	0.00	0.14	0.20	0.14	0.02	99.24	0.936
Kytlym	Kosva	37.82	0.03	0.00	20.20	39.43	1.46	0.04	0.01	0.02	0.21	0.00	0.00	0.00	99.22	0.777
Kytlym	Butyrin vein	40.55	0.01	0.00	11.45	48.61	0.24	0.01	0.00	0.00	0.01	0.00	0.00	0.00	100.88	0.883
Kachkanar	Svetily Bor	41.17	0.00	0.00	7.98	49.45	0.21	0.03	0.00	0.00	0.00	0.17	0.12	0.00	99.13	0.917
Kachkanar	Svetily Bor	41.49	0.00	0.24	7.40	49.96	0.15	0.03	0.00	0.00	0.00	0.12	0.14	0.02	99.54	0.923
Nizni Tagil	Solovieva	40.74	0.02	0.04	6.97	51.24	0.08	0.28	0.00	0.00	0.00	0.11	0.00	0.00	99.48	0.929
Nizni Tagil	Solovieva	40.39	0.02	0.00	7.44	50.88	0.18	0.27	0.00	0.00	0.00	0.17	0.00	0.00	99.35	0.924
Nizni Tagil*	Solovieva	41.04	0.03	0.03	4.33	53.41	0.06	0.24	0.00	0.00	0.46	0.16	0.00	0.00	99.76	0.956
Nizni Tagil	Gosshkhta	42.15	0.00	0.00	3.57	53.12	0.11	0.26	0.00	0.00	0.80	0.14	0.00	0.00	100.15	0.964
Uktus	S-dunite	42.98	0.00	0.00	2.58	53.61	0.11	0.02	0.00	0.00	0.09	0.43	0.00	0.03	99.85	0.974
Uktus	S-dunite	40.90	0.00	0.02	11.88	47.36	0.20	0.18	0.05	0.00	0.17	0.17	0.00	0.01	100.93	0.877
Uktus	N-dunite	40.59	0.00	0.00	13.97	45.67	0.24	0.07	0.00	0.00	0.00	0.12	0.00	0.02	100.68	0.854
Uktus	N-dunite	40.10	0.01	0.00	14.26	44.82	0.26	0.07	0.09	0.00	0.02	0.07	0.07	0.03	99.81	0.849

(*) = olivine inclusion in Chromite.

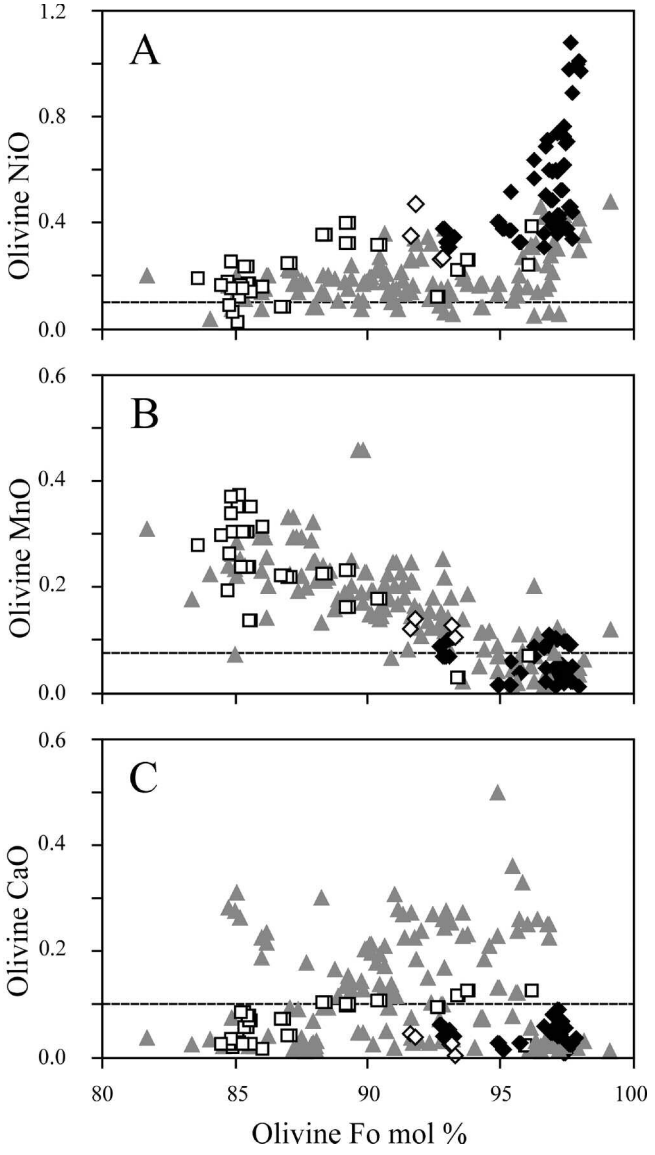

Fig. 13 - Variation of NiO, MnO, and CaO as functions of forsterite molar % in accessory olivine from chromitites of the Urals. Black diamond: podiform chromitite in ophiolitic mantle tectonite (Kempirsai, Kraka, Kluchevskoy, Ray-Iz). Open diamond: stratiform chromitite in supra-Moho cumulates of Kempirsai. Open square: stratiform chromitite in dunite of the East-Khabarny layered intrusion. Grey triangle: Syngenetic and epigenetic chromitite from Ural-Alaskan type complexes. Horizontal dashed line represents the approximate position of the average detection limit. Sources of data: Thalhammer (1996), Melcher et al. (1999), Pushkarev (2000), Garuti et al. (2003), Zaccarini (2005), Krause et al. (2007), Pushkarev et al. (2007), Zaccarini et al. (2008, 2011).

EPMA investigation of the olivine composition in a great number of chromitites of the Urals (Zaccarini, 2005) has revealed that fine-grained olivine inclusions in chromite have a higher forsterite and NiO content compared with olivine in large interstitial patches.

Oxygen thermo-barometric data

Detailed studies of chromite-olivine thermometry and oxygen barometry in chromitites of the Urals can be found in Chashchukhin et al. (1996; 2002; 2007), Pushkarev (2000), Pushkarev and Anikina (2002), Garuti et al. (2003), Zaccarini (2005), and Pushkarev et al. (2007). Thermo-barometric data reported here were obtained by the various authors using the equations of Ballhaus et al. (1991) at a constant pressure of 10 kb. The oxygen fugacity is expressed as $\delta\log f(O_2)$, e.g., deviation from the Fayalite-Magnetite-Quartz (FMQ) buffer.

The ophiolitic chromitites cover a wide range of calculated temperatures from 1510° to 590°C, and oxygen fugacities from -1.7 to + 2.73 $\delta\log f(O_2)$. Most of the mantle-hosted chromitites yield temperatures from 1291° to 640°C and oxygen fugacities above FMQ (Fig. 14A). Only a few samples from the mantle tectonite of Kempirsai give oxygen fugacities below the FMQ buffer and very high temperatures above 1200°C (Chashchukhin et al., 1996; 2007). The High-Al chromitites give temperatures below ~ 1000°C, at oxygen fugacities between -0.1 and +2.2 $\delta\log f(O_2)$. The supra-Moho cumulus chromitites cover a thermal range of 1230-760°C, at oxygen fugacities between -0.2 and +2.3, excluding one anomalous value of +4.7 from Voykar-Synynsky. Compared with ophiolitic chromitites, chromitites from East-Khabarny and Ural-Alaskan complexes are characterized by much higher values of oxygen fugacity from +2.1 to +5.9 $\delta\log f(O_2)$. They split into two different temperature ranges of 1490-930°C and 1025-600°C according to their syngenetic or epigenetic origin, respectively (Fig. 14A).

The whole set of calculated $\delta\log f(O_2)$ values displays a broad positive correlation with $Fe^{3+}/(Fe^{3+} + Fe^{2+})$ in chromite showing an increase in the oxidation state from chromitites in ophiolitic mantle to those in supra-Moho cumulates and Ural-Alaskan complexes (Fig. 14B).

Significance of chromite-olivine phase relations

Textural evidence arguing to olivine-chromite co-crystallization in the magmatic stage (e.g., the presence of olivine inclusions in chromite) is observed in all types of chromitite of the Urals. However, most of the temperatures obtained from the olivine-chromite equilibrium do not represent real liquidus temperatures. On the contrary, they reflect adjustment of the olivine-chromite Mg/Fe ratios in the post-magmatic stage and represent the closure temperature for the Fe-Mg exchange reaction. The exchange reaction involves diffusion of Fe from olivine into the oxide, the extent of exchange depending, among other factors, on the chromite/olivine mass ratio and the cooling rate (e.g., Irvine, 1967; Arai, 1980; Dick and Bullen, 1984; Ballhaus et al., 1991; Roeder, 1994). In massive chromitites (chromite volume > 90%), the chromite/silicate mass ratio tends to infinite, thereby the Fe diffusing from accessory olivine into the host chromite is extremely diluted, without causing perceptible changes of the primary Mg/Fe ratio in chromite. In contrast, the accessory olivine undergoes significant enrichment in Mg and all the other minor constituents (e.g., Ni). The forsterite content of accessory olivine increases irregularly depending on the grain size, and thereby in chromitites of the Urals. Small olivine inclusions usually have higher Mg# and Ni content compared with large aggregates interstitial to chromite (Zaccarini, 2005, and Table 4). A rapid cooling rate strongly reduces the chance of re-equilibration that, on the contrary, is enhanced by long lasting annealing under metamorphic conditions (Ozawa, 1984).

The Mg numbers in olivine and chromite show positive correlation over a wide range of values in groups of samples from individual ore bodies in ophiolite complexes (Fig. 15A), and the chromitites from East Khabarny and single Ural-Alaskan intrusions (Fig. 15B). The correlation trends

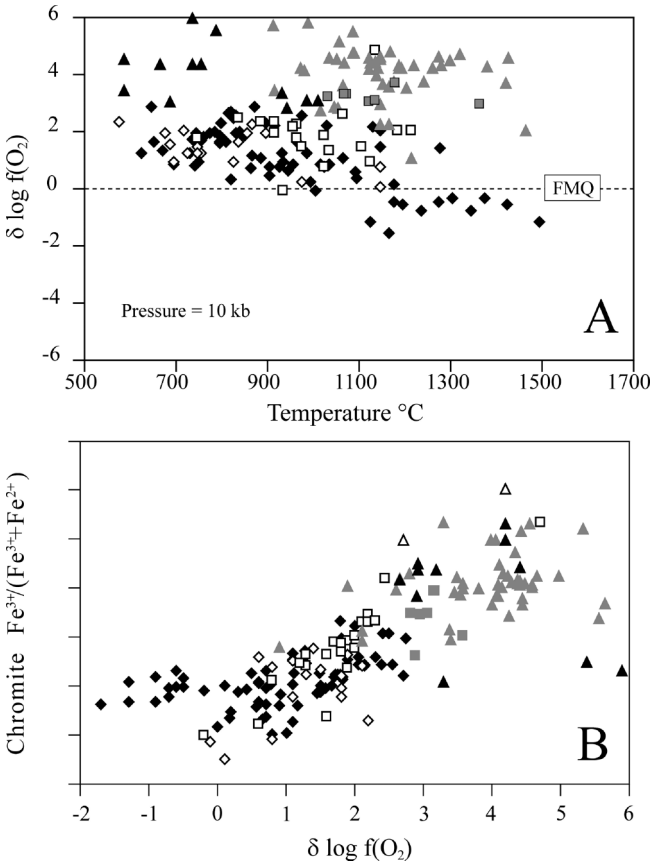

Fig. 14 - A) Oxygen fugacity and temperature calculated for 177 chromite-olivine pairs from the chromitites of the Urals. The horizontal dashed line represents the fayalite-magnetite-quartz (FMQ) buffer. B) Variation of the chromite oxidation ratio [$Fe^{3+}/(Fe^{3+} + Fe^{2+})$] as a function of the oxygen fugacity. Diamonds: high-Cr (black) and high-Al (open) podiform chromitite in ophiolitic mantle tectonite of Kempirsai, Kraka, Kluchevskoy, Ray-Iz, EastTagil, Alapaevskoy. Open square: stratiform chromitite in supra-Moho cumulates of Kempirsai and Voykar Syninsky. Grey square: stratiform chromitite in dunite of the East-Khabarny layered intrusion. Triangles: Syngenetic (grey) and epigenetic (black) chromitite from Ural-Alaskan type complexes. Sources of data: Chashchukhin et al. (1996, 2002, 2007), Pushkarev (2000), Pushkarev and Anikina (2002), Garuti et al. (2003), Zaccarini (2005), Pushkarev et al. (2007).

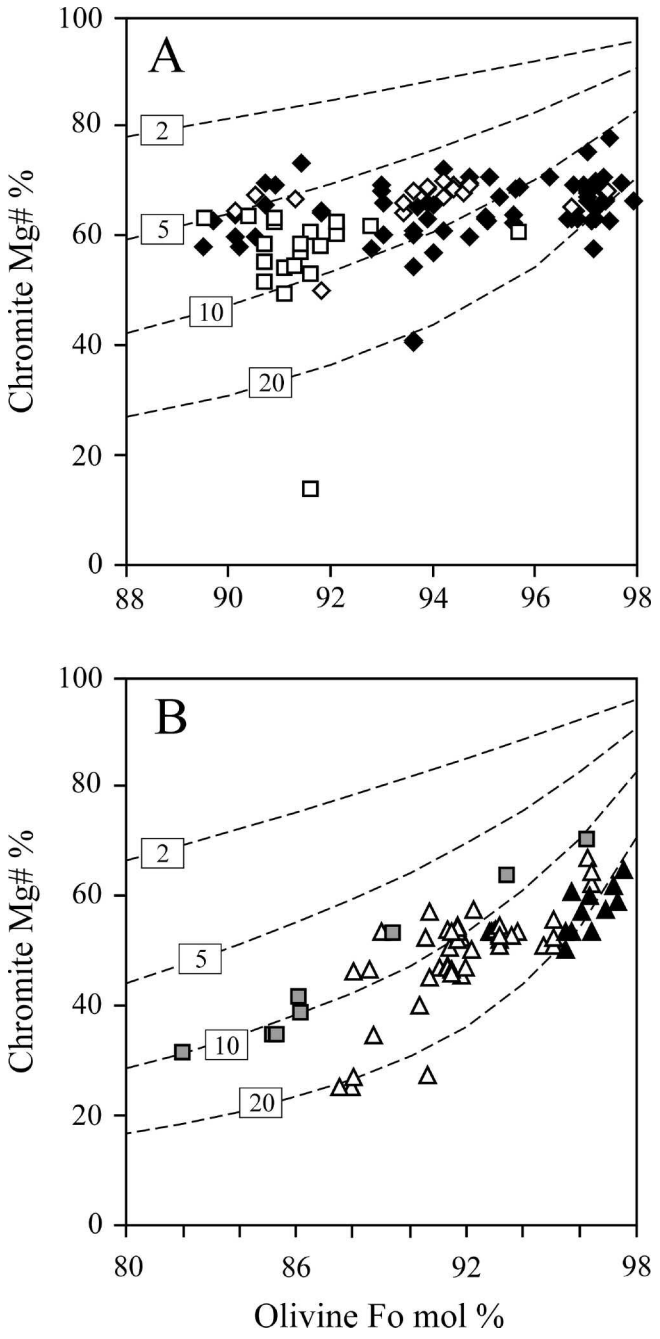

Fig. 15 - Relationships between forsterite content of accessory olivine and Mg# of host chromite for 175 chromite-olivine pairs from the chromitites of the Urals. A) Ophiolite complexes, diamonds: high-Cr (black) and high-Al (open) podiform chromitite in ophiolitic mantle tectonite of Kempirsai, Kraka, Kluchevskoy, Ray-Iz, East Tagil, Alapaevskoy. Open square: stratiform chromitite in supra-Moho cumulates of Kempirsai and Voykar Syninsky. B) Ural-Alaskan type intrusions, triangles: syngenetic chromitite (white), epigenetic chromitite (black). East-Khabarny: grey square. The dashed lines are the Kd = $(Mg/Fe)_{ol}/(Mg/Fe^{2+})_{chr}$ isopleths calculated for Kd = 2, 5, 10, 20 (numbers in boxes). See text for explanation.

broadly parallel the Kd = $(Mg/Fe)_{ol}/(Mg/Fe^{2+})_{chr}$ isopleths between Kd = ~ 8 and Kd = 20 in most cases. This feature suggests that sub-solidus re-equilibration of the Mg/Fe distribution between olivine and chromite occurred, but did not obliterate the primary relationship (Chashchukhin et al., 1996; Garuti et al., 2003), still indicating co-crystallization of the two phases from differentiating melts.

COMPARISON OF THE URAL CHROMITITES WITH SPINELS FROM DIFFERENT MAGMATIC SUITES AND AN ESTIMATE OF THEIR PARENTAL MELT COMPOSITION

Since the pioneer papers of Irvine (1965; 1967), it was established that the composition of chrome spinel from igneous rocks can be used as a guide to the chemistry of mantle-derived magmas and degree of partial melting of the mantle source, thus providing indirect indication of the geodynamic affinitity of the host magmatic rocks (Hill and Roeder, 1974; Evans and Frost, 1975; Dick and Bullen, 1984; Arai, 1992; Roeder 1994; Barnes and Roeder, 2001). Experimental data for chromite-melt equilibrium (Maurel and Maurel, 1982; Maurel, 1984; Ulmer, 1989; Roeder and Reynolds, 1991) have demonstrated a close relationship between the Al_2O_3, TiO_2, MgO and FeO contents of chromite and concentrations of these oxides in the melt in equilibrium with chromite. Recently, Kamenetsky et al. (2001) have

shown that accessory spinels from different magmatic suites define distinct compositional fields in an Al_2O_3-TiO_2 diagram, according to their different geodynamic settings of formation.

The study of chromitites has indicated that ophiolitic chromitites, on average, have lower TiO_2 contents (< 0.30 wt%) compared with chromitites in layered intrusions (e.g., Dickey, 1975; Mussalam et al., 1981; Ferrario and Garuti, 1988; Barnes and Roeder, 2001; Garuti, 2004; Zaccarini et al., 2004b; 2008; Zaccarini, 2005). Podiform chromitites from SSZ- and MOR-peridotites usually are of the high-Cr and high-Al variety, respectively, and in general, the high-Cr chromitites have lower TiO_2 compared with the high-Al types (Leblanc and Nicolas, 1992; Zhou and Bai, 1992; Zhou et al., 1994; Robinson et al., 1997; Proenza et al., 1999; Rollinson, 2008; Uysal et al., 2009; Escayola et al., 2011). Furthermore, chromitites from SSZ- and MOR-peridotites have lower TiO_2 compared with chromitites in sub-continental mantle (Gervilla and Leblanc, 1990; Garuti, 2004; Zaccarini et al., 2004a).

In this chapter, we compare the average compositions of different types of chromitite from the Urals with the Al_2O_3-TiO_2 compositional fields of accessory spinels from different volcanic suites (Table 5), and chromitites from plutonic associations, namely: i) mantle peridotites from supra-subduction zone, mid-oceanic-ridge, and sub-continental deep crust, ii) continental layered intrusions, and iii) concentric-zoned complexes of the Russian Far East (Table 6). Finally, using the empirical expressions of Maurel (1984) in Augé (1987) and Rollinson (2008), we have calculated the composition of melts parental to the chromitites in terms of Al_2O_3 and TiO_2 contents and FeO/MgO ratio (Table 7). The results of these calculations are compared with the fields of mafic magmas formed in different geodynamic settings.

Comparison with spinels in volcanic suites

The high-Cr podiform chromitites from the ophiolitic mantle plot in the field of low-Ti island-arc boninites and

Table 5 - Compositions of chrome spinels in various volcanic suites.

	TiO_2	Al_2O_3	Fe_2O_3	FeO	MnO	MgO	Cr_2O_3	FeOtot	FeO/MgO	Cr#	FeO/MgO
Mid oceanic ridge basalt (MORB), Cr# <0.70											
FAMOUS, MAR/2	0.28	27.47	4.33	10.60	0.15	16.88	40.29	14.50	0.63	0.50	0.63
54°S, MAR/3	0.23	31.07	4.31	10.58	0.08	17.06	35.59	14.46	0.62	0.44	0.62
54°S, MAR/3	0.20	34.85	4.29	9.94	0.11	17.96	32.83	13.80	0.55	0.39	0.55
43°N MAR (Ali 32 12-2)/4	0.39	20.84	4.36	11.17	0.11	15.75	47.04	15.10	0.71	0.60	0.71
43°N MAR (Ali 32 11-92)/4	0.51	19.41	4.99	11.15	0.13	15.65	47.70	15.65	0.71	0.62	0.71
Macquarie Island/6	0.38	28.51	5.11	11.10	0.14	16.63	38.21	15.70	0.67	0.47	0.67
Macquarie lsiand (40428)/6	1.47	20.91	9.23	16.49	0.18	12.48	36.99	24.81	1.32	0.54	1.32
Macquarie lsiand (60596)/6	0.70	25.20	6.74	13.87	0.12	14.34	37.74	19.94	0.97	0.50	0.97
Macquaríe lsiand (38324)/6	1.26	25.21	9.34	14.51	0.09	14.15	33.69	22.92	1.03	0.47	1.03
Macquarie Islanci (38159)/6	0.65	30.48	6.35	11.77	0.20	16.34	33.61	17.49	0.72	0.43	0.72
Macquarie Islanci (60701)/6	0.56	33.58	5.89	11.45	0.12	16.86	30.84	16.76	0.68	0.38	0.68
Gorda Ricige, E. Pacífic	0.43	28.97	5.66	12.35	0.17	15.93	36.12	17.45	0.78	0.46	0.78
Hole 896A, E. Pacific	0.36	29.10	6.33	11.65	0.16	16.40	36.01	17.35	0.71	0.45	0.71
Vema FZ, MAR	0.16	38.96	5.64	8.72	0.13	19.12	26.79	13.80	0.46	0.32	0.46
Galapagos Alvín 1549-5	0.39	27.15	6.67	13.52	0.10	14.94	37.24	19.53	0.90	0.48	0.90
Galapagos All 60 9/20	0.33	36.71	4.82	10.06	0.13	18.29	30.49	14.40	0.55	0.36	0.55
Snaefelisnes, Iceland	0.91	23.67	7.74	13.94	0.19	14.60	38.40	20.91	0.95	0.52	0.95
Hunter Ridge-Hunter FZ (IAT)	1.00	24.92	7.86	15.36	0.25	13.88	36.90	22.44	1.11	0.50	1.11
Back-arc basalt (BAB), Cr# < 0.70											
Southern North Fiji Basin/7	0.41	35.96	5.16	10.69	0.14	17.81	29.87	15.34	0.60	0.36	0.60
Oceanic-island basalt (OIB), Cr# <0.70											
Mauna Loa, Hawaii	1.39	14.14	9.07	16.40		12.24	45.85	24.57	1.34	0.68	1.34
Island-arc, high-K and calc-alkaline basalt (IAB), Cr# > 0.70											
Tumrok, E. Kamchatka/13	0.28	10.93	10.51	12.03	0.18	13.71	50.86	21.50	0.88	0.76	0.88
Tumrok, E. Kamchatka/13	0.29	8.72	11.82	12.51	0.23	13.54	51.90	23.16	0.92	0.80	0.92
Valaginsky, E. Kamchatka/13	0.44	7.70	18.32	13.04	0.22	13.19	46.54	29.54	0.99	0.80	0.99
Vulsini, Roman Province/14	0.49	15.34	6.08	12.29	0.22	14.59	50.96	17.77	0.84	0.69	0.84
Vulcano, Aeolian arc/15	0.55	8.68	16.23	15.33	0.29	12.02	47.92	29.95	1.28	0.79	1.28
Island-arc boninite and tholeite basalt (IABon IAT), Cr# > 0.70											
Cape Vogel, Papua New Guinea/19	0.04	2.92	3.82	8.75	0.13	15.29	68.64	12.19	0.57	0.94	0.57
Hunter Ridge-Hunter FZ/20	0.19	5.22	7.98	14.73	0.24	11.80	59.96	21.92	1.25	0.86	1.25
Koryak highland, E. Russia	0.08	10.37	5.00	13.16	0.21	13.40	57.79	17.66	0.98	0.79	0.98
E. Valu Fa Ridge, Lau Basin/12	0.28	7.70	7.58	11.04	0.16	14.32	58.18	17.87	0.77	0.84	0.77
Large igneous provinces (LIP): Flood Basalts, Cr#>70											
Karoo, South Africa/29	3.68	8.33	7.29	20.94	0.23	9.86	49.36	27.51	2.12	0.80	2.12
Emeishan, SW China/30	3.57	9.72	16.17	24.58	0.28	7.52	38.42	39.15	3.27	0.73	3.27
Central Siberia Plateau/31	3.85	6.25	12.09	15.16	0.15	13.53	48.62	26.05	1.12	0.84	1.12
Nuussuaq, W. Greenfancl/32	0.97	18.57	9.55	16.22	0.28	12.27	40.91	24.82	1.32	0.60	1.32

Data sources: Kamenetsky et al. (2001).

Table 6 - Average compositions of chrome spinels in various chromitites from plutonic associations.

Host Complex (ref.)	details	n° an.	TiO_2	Al_2O_3	FeO	Fe_2O_3	MgO	MnO	Cr_2O_3	Fe^{2+}#	Cr#
Spinel in Abyssal peridotites (2)											
Islas Orcadas		21	0.04	48.76	10.04	2.67	19.03	0.09	18.37		0.20
MAR-43°N			0.05	25.08	13.77	3.68	14.04	0.12	41.54		0.53
Chromitite in ophiolitic mantle (4, 7, 8, 9, 10)											
Vourinos	high-Al	13	0.16	25.45	12.08	3.93	15.44	0.25	42.69	0.31	0.53
Vourinos	high-Cr	80	0.14	11.28	12.98	3.61	13.34	0.30	58.35	0.35	0.78
Troodos	high-Al	11	0.19	23.55	12.26	4.02	15.32	0.17	44.49	0.31	0.56
Troodos	high-Cr	66	0.15	14.87	12.75	3.70	14.09	0.18	54.26	0.34	0.71
Albania	high-Al	13	0.15	27.93	10.84	4.29	17.10	0.24	39.45	0.26	0.49
Albania	high-Cr	52	0.13	10.96	12.68	3.62	13.85	0.25	58.51	0.34	0.78
Turkey	high-Al	11	0.18	26.07	11.94	3.44	15.75	0.17	42.45	0.30	0.52
Turkey	high-Cr	96	0.16	12.01	12.28	3.15	14.03	0.53	57.84	0.33	0.76
Oman	high-Al	22	0.35	25.11	13.78	3.26	14.53	0.28	42.69	0.35	0.53
Oman	high-Cr	11	0.17	15.33	12.61	3.22	14.18	0.32	54.17	0.33	0.70
Philippines	high-Al	21	0.21	25.27	14.37	5.18	14.10	0.00	40.87	0.36	0.52
Philippines	high-Cr	28	0.00	11.89	16.05	4.70	11.58	0.00	55.78	0.44	0.76
China	high-Al	15	0.26	22.17	14.00	3.31	13.89	0.30	46.07	0.36	0.58
China	high-Cr	25	0.17	15.35	12.98	2.93	12.71	0.47	55.39	0.36	0.71
Cuba	high-Al	24	0.29	29.40	11.61	3.66	16.43	0.20	38.41	0.28	0.47
Cuba	high-Cr	5	0.19	14.36	12.31	3.30	14.34	0.21	55.29	0.33	0.72
New Caledonia	high-Al	9	0.14	25.80	10.98	2.64	16.40	0.15	43.89	0.27	0.53
New Caledonia	high-Cr	32	0.07	15.20	11.92	2.92	14.62	0.22	55.05	0.31	0.71
Chromitite in subcontinental mantle (4, 6, 9, 10)											
Finero	high-Cr	75	0.42	18.07	16.92	4.60	11.87	0.23	47.35	0.59	0.72
Ronda	high-Al	200	0.38	28.38	24.00	0.97	8.03	0.29	36.48	0.75	0.56
Chromitite in continental layered intrusions (3, 4, 5, 10)											
Bushveld	LG-MG-UG-Layers	210	0.91	15.70	21.02	7.82	8.96	0.30	44.73	0.70	0.74
Bushveld	MR	20	0.90	15.27	19.98	8.64	9.55	0.29	44.78	0.68	0.75
Bushveld	Pipes	45	1.32	18.57	25.38	2.12	6.74	0.35	44.91	0.79	0.71
Great Dyke	av. of all layers	80	0.54	15.28	17.85	3.76	10.87	0.30	50.88	0.62	0.77
Stillwater	Layer A	10	2.11	19.93	28.74	5.86	5.05	0.25	35.96	0.85	0.64
Stillwater	average of 7 layers	88	0.56	18.97	18.82	7.58	10.58	0.32	42.72	0.64	0.69
Campo Formoso	average of 7 layers	62	0.19	14.39	18.19	5.15	10.16	0.39	51.28	0.64	0.78
Niquelandia	average of 2 layers	102	0.33	24.73	16.74	2.90	12.25	0.17	42.77	0.58	0.63
Chromitite in Alaskan-type complexes of Russian-Far-East (1, 4)											
Galmoenan (Kamchatka island arc)		10	0.42	6.97	19.06	17.75	8.90	0.58	46.32	0.68	0.87
Kondyor (Russian-Far-East craton)		40	0.74	5.77	16.39	14.26	11.16	0.39	52.61	0.59	0.90

Data sources: 1) Chaschukhin et al. (2007); 2) Dick and Bullen (1984); 3) Ferrario and Garuti (1988); 4) Garuti (2004) database; 5) Garuti et al. (2007); 6) Gervilla and Leblanc (1990); 7) Proenza et al. (1999); 8) Uysal et al. (2010) databse; 9) Zaccarini et al. (2004a); 10) Zaccarini (2005) database.

tholeiites (IAB, IAT), whereas the high-Al variety is shifted towards the field of MORB (Fig. 16A). Some of the high-Al stratiform chromitites from the supra-Moho cumulates of Kempirsai, Voykar Syninsky, Ray-Iz and Nurali enter the field of spinels in modern MORB lavas (e.g., Mid-Atlantic Ridge, Iceland, Macquarie Islands SW Pacific, Galapagos E Pacific) and back-arc basin basalts (BABB) of the Fiji basin (Fig. 16B). However, most compositions, including the CHR-1 samples, have TiO_2 lower than in MORB spinels, at a comparable concentration of Al_2O_3. Notably, compositions from the Nurali CHR-2 layer plot in an area overlapping those of spinels from high-Ti-K IAB, MORB and flood basalts from West Greenland (Larsen and Pedersen, 2009). The stratiform chromitites from East-Khabarny form a unique cluster with the Ural-Alaskan type chromitites (Fig. 16C) overlapping the field of spinels from high-Ti-K IAB (including ankaramitic lavas) and calc-alkaline volcanic series of the East Kamchatka, Roman and Aeolian volcanic provinces. The epigenetic chromitites spread over a wide range of TiO_2 contents (0.37-3.4 wt%) at very low Al_2O_3 (3.5-15.1 wt%). Samples from the Butyrin veins of Kytlym have the highest TiO_2 concentrations (2.7-3.4 wt%), being similar to spinels in continental flood basalts from the large igneous provinces (LIP) (Central Siberian Plateau, SW China Emeishan, and South Africa Karoo).

Comparison with chromitites in ultramafic plutonic associations

Podiform and stratiform chromitites from ophiolites of the Urals plot in the field of spinels from SSZ peridotite or are shifted towards the MOR-peridotite field, according to their high-Cr or high-Al compositions, respectively (Fig. 17A). The only exception are chromite compositions from the CHR-2 chromitite layer of Nurali that are shifted to higher TiO_2 contents, entering the field of chromitites of the sub-continental mantle massifs of Finero (Western Alps) and Ronda (Betic Cordillera). The CHR-2 samples also have relationships comparable with those observed in chromitites of major continental layered intrusions (Fig. 17B), in contrast to the other stratiform chromitites of the Urals that mostly are shifted towards the low-TiO_2 high-Al_2O_3 field of MORB spinels. The East-Khabarny and Ural-Alaskan chromitites have a similar range of TiO_2 as shown by the Bushveld and Stillwater chromitites, but are comparatively depleted in Al_2O_3 (Fig. 17B). Compositions of chromitites from the concentrically zoned intrusion of Galmoenan (Kamchatka island arc) plot in the Al_2O_3-poor side of the East-Khabarny and Ural-Alaskan field. However, samples from Kondyor (Russian Far East craton) enter the field of the Ural samples, implying derivation from similar melts despite of the different geodynamic setting (Fig. 17C).

Table 7 - Composition of chromite and calculated parental melts for chromitites of the Urals compared with volcanic suites.

			Chromite									Melt		
Host Complex	n° anal.	Ore Type	TiO_2	Al_2O_3	FeO	Fe_2O_3	MgO	MnO	Cr_2O_3	Fe^{2+}#	Cr#	FeO/MgO	*Al_2O_3	*TiO_2	**FeO/MgO
Ophiolitic mantle															
Voykar Syninsky	10	high-Cr	0.14	9.66	14.07	5.37	12.19	0.10	57.38	0.39	0.80	1.15	10.78	0.23	0.85
Voykar Syninsky	25	high-Al	0.14	22.63	10.78	5.67	16.46	0.01	42.96	0.27	0.56	0.65	15.06	0.46	0.61
Verkhneivinsky	1	high-Cr	0.14	8.66	16.34	0.00	10.99	0.33	63.55	0.45	0.83	1.49	10.21	0.23	1.11
Verkhneivinsky	2	high-Al	0.15	17.59	12.34	2.63	14.60	0.26	52.43	0.32	0.67	0.85	13.91	0.24	0.73
Ray-Iz	46	high-Cr	0.10	9.71	12.23	4.45	13.70	0.26	59.17	0.33	0.80	0.89	10.81	0.19	0.66
Ray-Iz	46	high-Al	0.19	16.03	12.33	4.38	14.46	0.18	52.29	0.32	0.69	0.85	13.43	0.30	0.71
Kempirsai	150	high-Cr	0.16	10.08	11.03	4.55	14.62	0.28	59.18	0.30	0.80	0.75	11.01	0.25	0.56
Kraka	41	high-Cr	0.17	13.15	11.55	4.83	14.62	0.22	55.29	0.31	0.74	0.79	12.39	0.27	0.62
Kluchevskoy	58	high-Cr	0.19	11.54	14.03	5.20	12.80	0.30	55.80	0.38	0.76	1.10	11.71	0.29	0.83
EastTagil	2	high-Cr	0.24	22.36	12.02	1.79	15.35	0.29	47.96	0.31	0.59	0.78	15.02	0.65	0.74
Alapaevskoy	1	high-Cr	0.32	10.15	12.19	4.73	13.98	0.31	58.32	0.33	0.79	0.87	11.04	0.45	0.65
Alapaevskoy	12	high-Al	0.26	23.78	12.60	3.95	15.13	0.25	44.03	0.32	0.55	0.83	15.24	0.69	0.80
Ophiolitic Supra-MOHO cumulates															
Voykar Syninsky	1	high-Cr	0.34	10.47	14.41	2.56	12.65	0.23	59.35	0.39	0.79	1.14	11.20	0.47	0.87
Voykar Syninsky	5	high-Al	0.38	26.16	18.05	5.01	11.83	0.27	38.15	0.46	0.49	1.53	15.59	0.86	1.53
Ray-Iz	5	high-Al	0.14	25.40	15.29	3.35	13.02	0.15	42.54	0.40	0.53	1.17	15.48	0.46	1.16
Kempirsai	53	high-Al	0.15	26.14	14.33	5.16	14.05	0.27	39.70	0.36	0.50	1.02	15.59	0.48	1.01
Nurali CHR-1	41	high-Al	0.07	28.94	12.98	5.45	15.23	0.20	36.78	0.32	0.46	0.85	15.97	0.29	0.88
Nurali CHR-2	43	high-Al	0.78	19.50	20.90	15.18	9.36	0.32	33.50	0.56	0.54	2.23	14.53	1.36	1.85
Ural-Alaskan type complexes															
Khabarninsky	158	syngenetic	0.70	10.21	17.93	10.52	10.35	0.40	49.61	0.49	0.77	1.73	11.07	0.83	1.24
Kachkanar	62	syngenetic	0.50	7.68	16.48	13.25	10.82	0.38	50.65	0.46	0.82	1.52	9.59	0.64	1.01
Kytlym	72	syngenetic	0.80	10.42	16.66	18.41	11.15	0.31	41.93	0.46	0.73	1.49	11.18	0.92	1.00
Nizhny Tagil	65	syngenetic	0.42	7.77	15.47	12.80	11.44	0.35	51.50	0.43	0.82	1.35	9.65	0.55	0.90
Uktus	170	syngenetic	0.84	12.10	18.25	14.43	10.32	0.35	43.30	0.50	0.71	1.77	11.96	0.95	1.27
Nizhny Tagil Gosshakhta	35	epigenetic	0.51	7.45	16.56	14.71	10.75	0.47	49.55	0.46	0.82	1.54	9.43	0.64	1.00
Kytlym Butyrin vein	43	epigenetic	2.82	5.84	27.16	30.22	4.85	0.50	28.41	0.76	0.77	5.60	8.16	2.48	3.05
Modern volcanic suites (1)															
MORB (Mid oceanic ridge basalt)	18	average of 18 local	0.57	28.17	12.12	6.09	15.96	0.14	36.47	0.43	0.56	0.76	15.99	1.10	0.91
BAB (Back-arc basalt)	1	S-N Fiji Basin	0.41	35.96	10.69	5.16	17.81	0.14	29.87	0.38	0.45	0.60	17.72	1.29	0.80
OIB (Oceanic-island basalt)	1	Mauna Loa, Hawai	1.39	14.14	16.40	9.07	12.24	0.00	45.85	0.57	0.76	1.34	11.93	2.19	0.85
IAB (Island-arc high-K, calc-alkaline basalt)	5	average of 5 localit	0.41	10.27	13.04	12.59	13.41	0.23	49.64	0.49	0.83	0.97	10.87	0.53	0.69
IABon IAT (Island-arc boninite, tholeite)	4	average of 4 localit	0.15	6.55	11.92	6.10	13.70	0.19	61.14	0.47	0.90	0.87	8.18	0.26	0.57
LIP (Large igneous provinces flood basalts)	3	average of 3 localit	3.02	10.72	19.23	11.28	10.80	0.24	44.33	0.64	0.81	1.78	7.98	3.39	0.81
W. Greenland flood basalt	1	Nuussuaq	0.97	18.57	16.22	9.55	12.27	0.28	40.91	0.57	0.69	1.32	14.69	1.84	1.36
Ankaramite (2)	7	average of 2 localit	0.55	10.63	15.09	12.73	12.25	0.29	48.38	0.55	0.82	1.23	9.65	0.69	1.03

(1) Kamenetsky et al. (2001), (2) Ortiz-Hernandez (2000), Elburg et al. (2007); n° anal. = number of averaged analyses for each ore type. Ore type: high-Cr = Cr# > 0.70, high-Al = Cr# < 0.70.
Calculated from the equations of *) Rollinson (2008) and **) Maurel (1987).

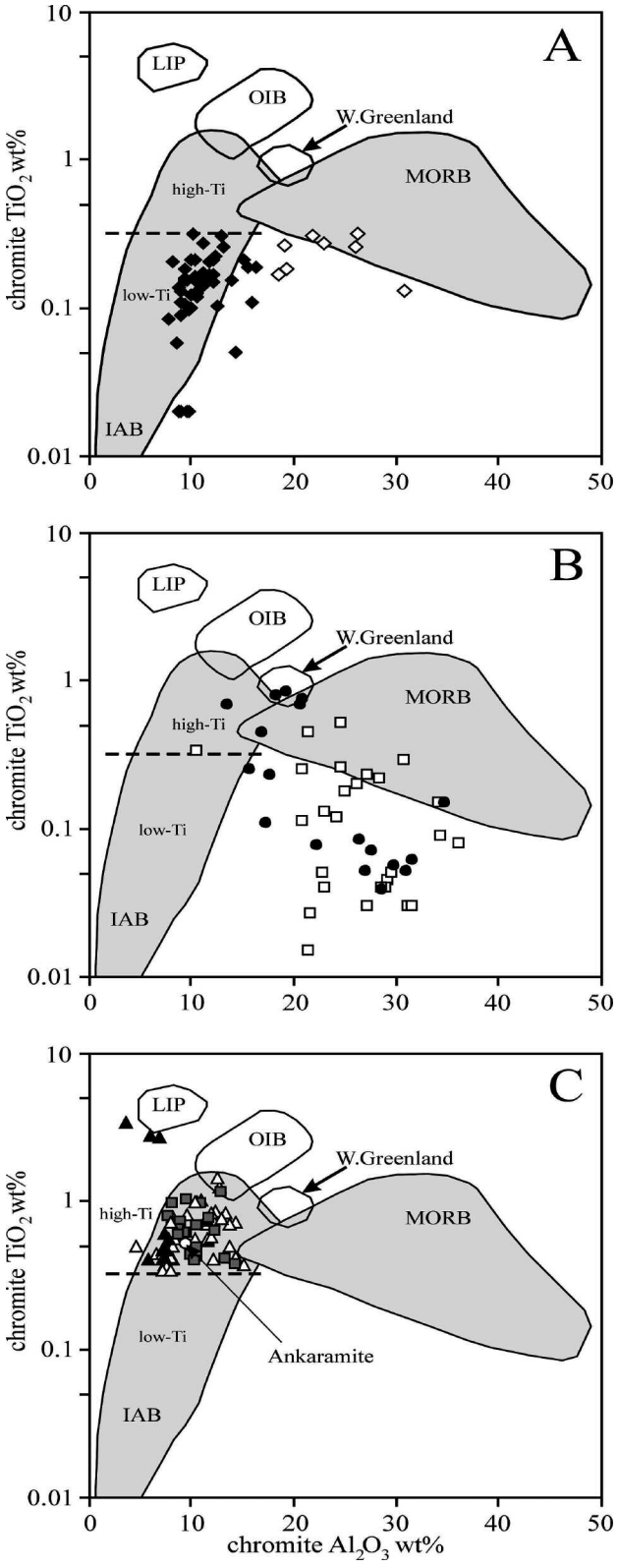

Fig. 16 - TiO_2-Al_2O_3 relationships in chromitites of the Urals, A) Mantle-hosted high-Cr (black diamond) and high-Al (open diamond) chromitites. B) Chromitites in supra-Moho cumulate sequences of the Urals, symbols: Kempirsai, Voykar Syninsky, Ray-Iz (open square), Nurali (black dot). C) Chromitites in Ural-Alaskan concentrically zoned complexes (open triangles: syngenetic, black triangle: epigenetic), and East-Khabarny (grey square), Average ankaramite (open circle) calculated from Ortiz-Hernandez (2000) and Elburg et al. (2007). The fields for IAB (island arc basalt), OIB (oceanic island basalt), MORB (mid-ocean ridge basalt), LIP (large igneous provinces) and W. Greenland flood basalt are from Kamenetsky et al. (2001). The dashed line at TiO_2 = 0.30 wt% separates high-Ti IAB (high-K calc-alkaline suite) from low-Ti IAB (boninite and low-Ti tholeiite suites).

Estimate of the chromitite parental melt composition

The calculated Al_2O_3, TiO_2 and FeO/MgO of melts parental to the Urals chromitites are compared with melt compositions of modern volcanic suites (Table 7). The significance of the calculated FeO/MgO is questionable since temperatures deduced from the olivine-chromite Fe-Mg exchange are much lower than magmatic temperatures in most cases. This limitation, however, is considered to be minimal in massive chromitites since the Fe-Mg exchange should affect only the composition of accessory olivine due to the high chromite/olivine volume ratio (Arai, 1980; Zaccarini, 2005). The concentrations of Al_2O_3 and TiO_2 in spinel are not significantly affected by post-magmatic equilibration with olivine, thus depending only on the parental melt composition (Kamenetsky et al., 2001).

The melts parental to ophiolitic chromitites reflect the bimodal character, high-Al and high-Cr, of the daughter chromites. Podiform chromitites hosted by the mantle section are predominantly of the high-Cr type and derived from melts having low Al_2O_3, TiO_2 and FeO/MgO consistent with island-arc boninite and tholeiite (Fig. 18A, B, C). In contrast, most of the stratiform chromitites from supra-Moho cumulate sequences pertain to the high-Al variety and were in equilibrium with MORB (Fig. 19A, B, C). In general, the results of the melt calculation are in broad agreement with the geologic settings proposed for major chromite deposits of the Urals (Melcher et al., 1997; 1999; Savelieva, 2004). There are, however, some apparent discrepancies concerning minor chromitite occurrences. For example, stratiform chromitites from Nurali seem to have derived from two different melts, with the melt parental to CHR-2 having too high FeO/MgO (Fig. 19C) for being of a MORB affinity. Furthermore, the melts calculated for the East-Khabarny and Ural-Alaskan type chromitites fit the ARC array in the Al_2O_3 diagram (Fig. 20A), but several samples have TiO_2 and FeO/MgO in excess compared with Al-poor melts generated in ARC settings, such as boninite, low-Ti tholeiite, high-K calc-alkaline basalt (Fig. 20B, C), and in one case (Kytlym Butyrin vein) they approach the TiO_2 content of intra-plate basalts (IPB).

MECHANISMS, TECTONIC SETTING, AND TIMING OF CHROMITITE FORMATION IN THE URALS

It is now currently accepted that chromitite forms by precipitation of chrome spinel from a mafic magma, in which chrome saturation was achieved and maintained long enough to allow precipitation of chrome spinel as the dominant liquidus phase. This condition is a result of the combination of various physical and chemical factors (temperature, pressure, oxygen fugacity, silica activity, hydrous fluids partial pressure etc.) by which the system is driven from the chromite-olivine cotectic line into the stability field of chromite (Fig. 21). Most common mechanisms involve mixing of evolved melts with more primitive magma or reaction between a fluid-rich percolating melt with country-rock peridotite (Irvine, 1977a; Zhou et al., 1994; Arai, 1997). In both cases, chromite crystallization can be enhanced, leading to the formation of economic-size deposits, if the reactants (mixing melts or interacting melt-rock) have a large degree of chemical disequilibrium (Zhou et al., 1994). When the reactants reach equilibrium, the reaction ceases and the composition of the melt is driven again to the

chromite-olivine cotectic line to produce disseminated ores (Fig. 21).

Chromitites of the Urals are typical examples of these mechanisms of formation. Their distribution through space and time indicates that chromitite-forming processes occurred repeatedly from the early phases of opening of the Uralian Ocean, in pre-Paleozoic or Early Paleozoic, to the development of an intra-oceanic subduction-island arc system, in Late Ordovician-Silurian times.

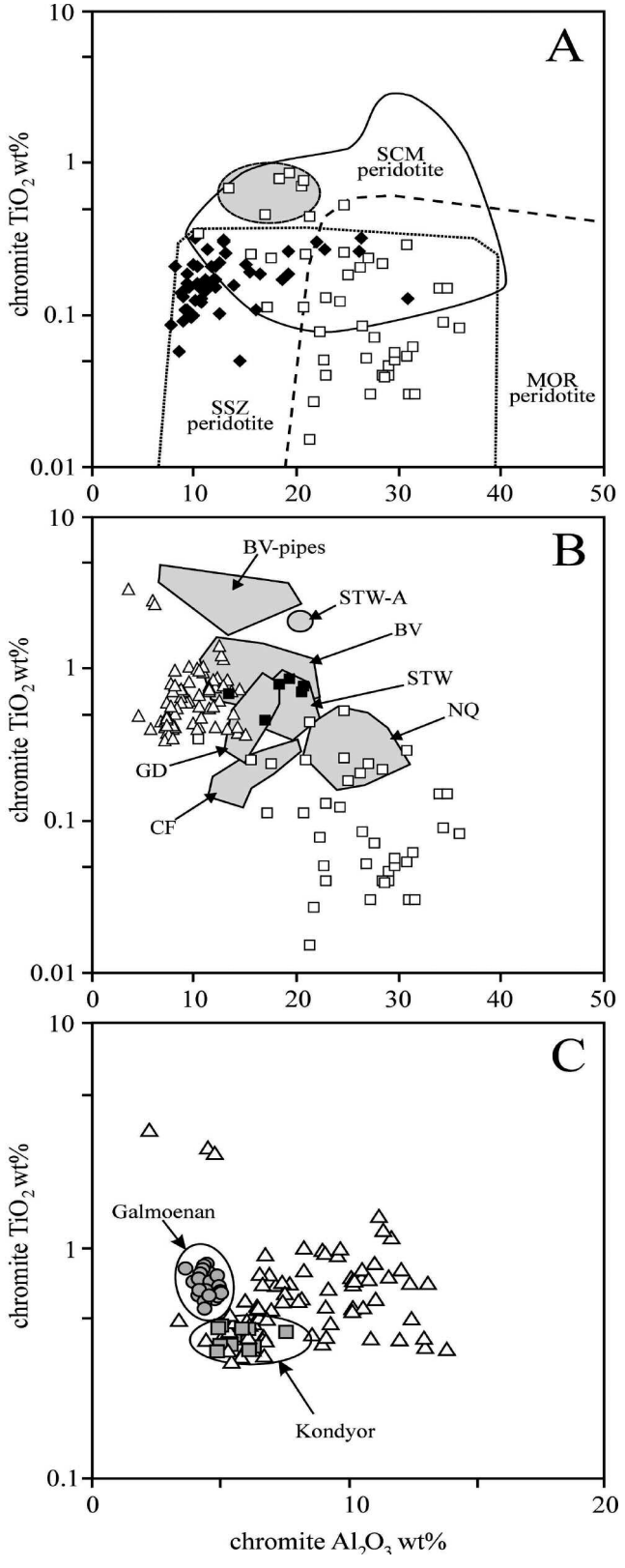

Fig. 17 - TiO_2-Al_2O_3 relationships in chromitites, A) Mantle-hosted (black diamond) and supra-Moho cumulate (open square) chromitites of the Urals, compared with the field of spinels from supra-subduction zone (SSZ) and mid-ocean ridge (MOR) mantle peridotites, and massive chromitite from the sub-continental mantle (SCM) of Finero (Western Alps) and Ronda (Betic Cordillera). The grey field includes the CHR-2 samples from Nurali. Data sources: Gervilla and Leblanc (1990), Kamenetsky et al. (2001), Garuti (2004), Zaccarini et al. (2004a, 2004b), Zaccarini (2005). B) East-Khabarny and Ural-Alaskan chromitites (open triangle), supra-Moho cumulate chromitites (open square), and CHR-2 layers of Nurali (black square) compared with the fields (in grey) of chromitites in continental layered intrusions; BV- Bushveld layered chromitite; BV-pipes-chromitite in platiniferous dunite pipes; STW- Stillwater layered chromitite; STW-A- Stillwater layer A (platiniferous); GD- Great Dyke; CF- Campo Formoso; NQ- Niquelandia. Data sources: Ferrario and Garuti (1988), Zaccarini et al. (2002), Garuti (2004), Zaccarini (2005), Garuti et al. (2007). C) East-Khabarny and Ural-Alaskan chromitites (open triangle) compared with chromitites from the concentrically zoned intrusions of Galmoenan in the Kamchatka island arc (grey circle) and Kondyor in the Russian Far East craton (grey square). Data sources: Chashchukhin et al. (2007), and unpublished data of the authors.

Podiform chromitites in ophiolitic mantle

Podiform chromitites in the ophiolitic mantle of the Urals represent the filling of magmatic conduits (Lago et al., 1982) and essentially formed by reaction between percolating melts and country-rock residual peridotite (Zhou and Robinson, 1994; Arai, 1997; Robinson et al., 1997). Isotopic and petrologic evidence from the Southern and Polar Urals (Melcher et al., 1999; Savelieva et al., 2007) indicates that high-Al and high-Cr chromitites formed in different stages during the evolution of the Uralian Ocean, involving emplacement in different geodynamic settings. The calculated compositions of melts in equilibrium with chromitite are consistent with this conclusion indicating that the high-Al and high-Cr types were derived from reaction of harzburgitic mantle with two distinct magmas having affinities of modern MORB and boninitic basalt, respectively.

The MORB-type melts were produced in nascent spreading centers at mid-ocean ridges or back-arc basins within the ancient Uralian Ocean. These melts derived from relatively low degrees of partial melting and, presumably, they were not far out of equilibrium with the wall-rock mantle harzburgite. For this reason, melt-rock reaction was probably limited (Bédard, 1989) generating chromite deposits of a small size and low Cr-grade. During progressive regression from the rifting zones, the sub-oceanic mantle underwent plastic flow and recrystallization, producing conformable fabrics in both the chromite ores and the host harzburgite. Based on the chromite-olivine geothermal data, the high-Al chromitites of the Urals underwent plastic flow at temperatures lower than ~ 800°C and oxygen fugacities of 1-2.3 log units above the FMQ buffer.

Boninitic magmas, such as those parental to the high-Cr, low-Ti chromitites of the Urals, are typically produced by melting of a depleted mantle source, at low pressures (< 10 kb) and high temperatures in a subduction influenced environment (Crawford et al., 1989; Falloon and Danyushevsky, 2000). These melts usually display a strong chemical disequilibrium, and therefore react intensively with the mantle harzburgite during their ascent. The melt becomes more siliceous by dissolution of the harzburgite orthopyroxene, and thereby its composition is shifted into the crystallization field of chromite. The country-rock peridotite is progressively enriched in Mg, giving rise to a dunite envelope.

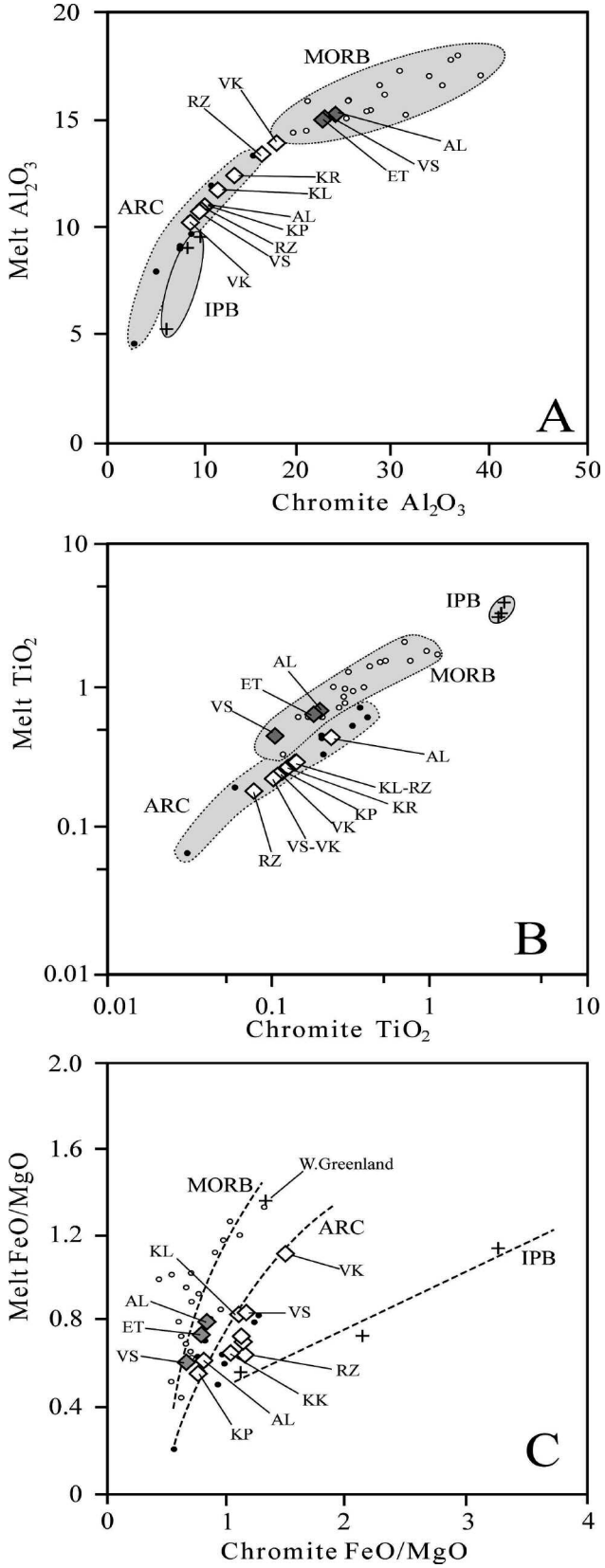

Fig. 18 - Chromite-melt relationships for A) Al_2O_3, B) TiO_2, and C) FeO/MgO, in high-Cr (open diamond) and high-Al (grey diamond) chromitites from the ophiolitic mantle of the Urals (Table 7). Labels: Al- Alapaevskoy; ET- East Tagil; KL- Kluchevskoy; KP- Kempirsai; KR- Kraka; RZ- Ray-Iz; VK- Verkhneivinsky; VS- Voykar Syninsky. MORB = white spot, ARC-lavas = black spot, and IPB intraplate basalts = (cross) are spinel-melt compositions (Table 5) from Kamenetsky et al. (2001). The grey fields for MORB, ARC, and IPB are drawn after regression-line equations from Rollinson (2008).

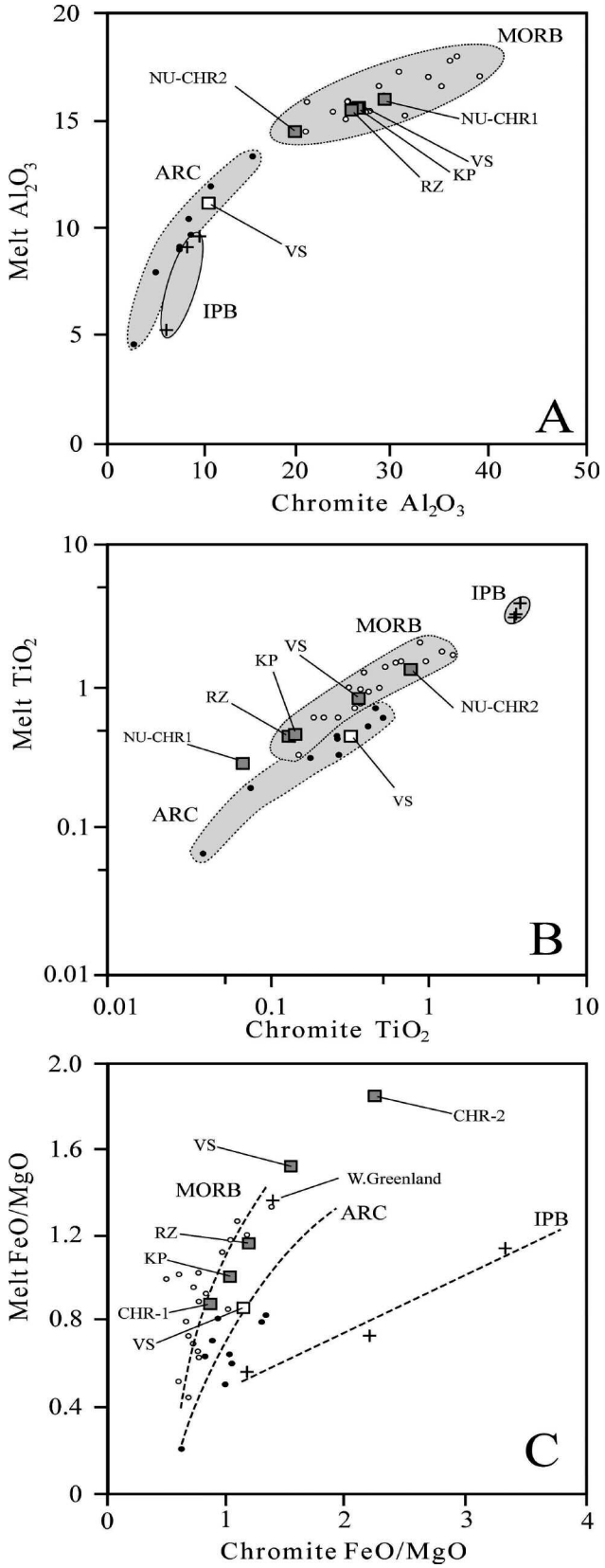

Fig. 19 - Chromite-melt relationships for A) Al_2O_3, B) TiO_2, and C) FeO/MgO, in high-Cr (open square) and high-Al (grey square) chromitites from supra-Moho cumulate sequences of the Urals. Labels: NU-CHR1 and NU-CHR2 data from Nurali, other labels and grey fields as in Fig. 18.

Continuous mixing of residual melt with newly injected boninitic magma contributes to maintain chromite as the sole liquidus phase, generating large deposits of massive, high-Cr chromitite, sheathed by metasomatic dunite (Robinson et al., 1997 and references therein). The chromite-olivine phase relations in high-Cr chromitites of the Urals indicate equilibration from extremely high temperatures (~ 1400°C) down to subsolidus conditions (< 800°C) with oxygen fugacities increasing from -1.7 log units below the FMQ buffer to +2.4 log units above it.

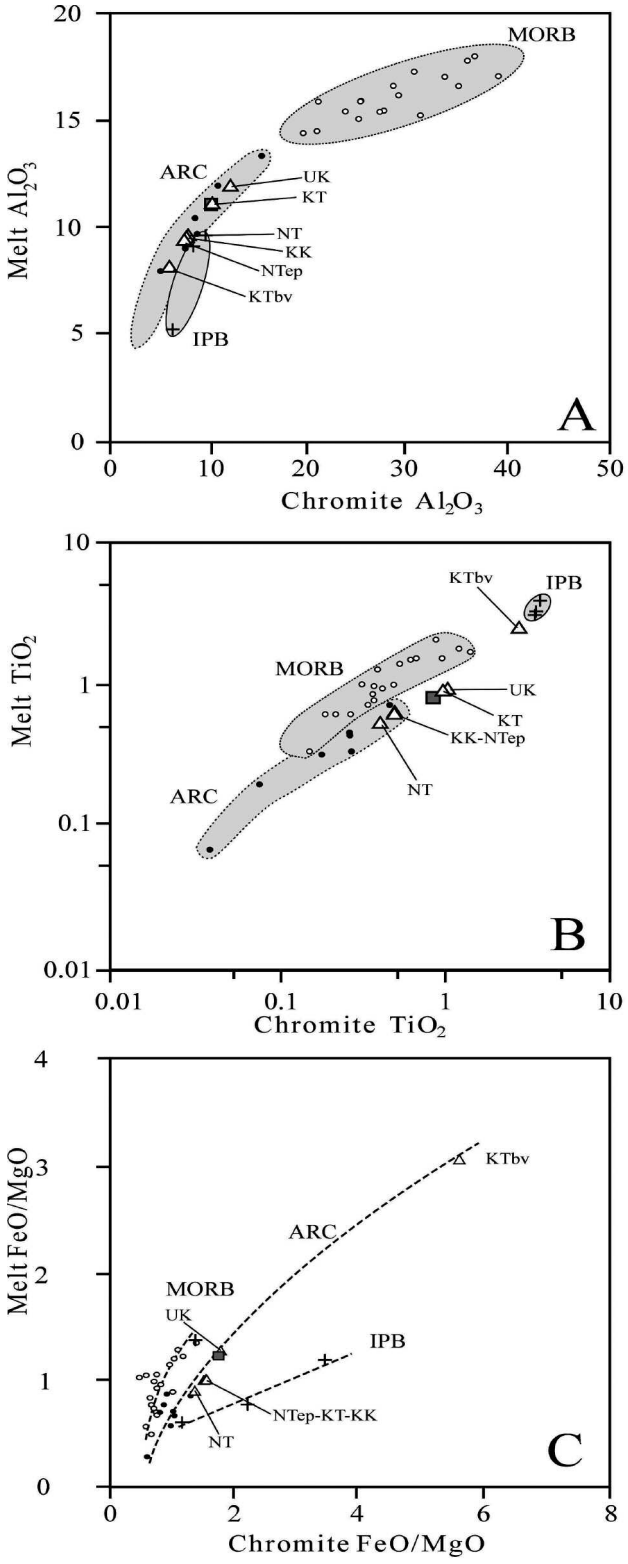

Fig. 20 - Chromite-melt relationships for A) Al_2O_3, B) TiO_2, and C) FeO/MgO, in chromitites from East-Khabarny (grey square) and Alaskan-type intrusions (open triangle) of the Urals. Labels: KK- Kachkanar; KT- Kytlym; NT- Nizhny Tagil; UK- Uktus; extension: bv- Butyrin vein; ep- epigenetic; other labels and grey fields as in Fig. 18.

Stratiform chromitites in supra-Moho ophiolitic cumulates

Supra-Moho cumulus sequences in ophiolite complexes of the Urals represent the product of fractional crystallization of melts intruded at and above the mantle-crust transition zone. Their predominant stratiform morphology, concordant with the layered structure of the host rocks, supports an origin by mixing-reaction between newly injected primitive melt and a chemically evolved resident liquid (Irvine, 1977a).

Melts parent to the stratiform high-Al chromitites of Kempirsai and Ray-Iz have MORB-like Al_2O_3 signature consistent with extrusion and emplacement in subduction-unrelated settings (Dilek and Furnes, 2011), possibly at spreading centers located west of the eastward-dipping, intraoceanic subduction (Melcher et al., 1997; Savelieva, 2004). However, several samples may have TiO_2 lower than typical MORB spinels at a given Al_2O_3 concentration. This feature is frequently observed when comparing volcanic spinels with spinels from plutonic rocks (Kamenetsky et al., 2001).

Stratiform chromitites in the layered sequence of Nurali seem to have crystallized in equilibrium with two different melts. The melt parental to CHR-1 was a low-Ti (TiO_2 = 0.30 wt%) and low-Cr tholeiite (Al_2O_3 > 14 wt%) with MORB-

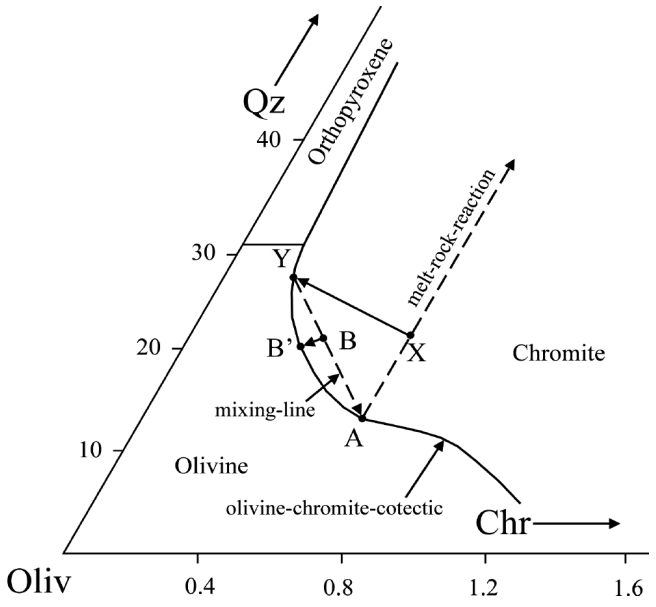

Fig. 21 - Mechanisms for chromitite formation according to phase relations in the ternary system Chromite-Olivine-Quartz (after: Irvine 1977b, Zhou et al. 1994, Robinson et al. 1997). 1) *The magma-mixing model*: fractionated melt Y forms melt B by mixing with primitive magma A. Due to an increase of silica activity, magma A is shifted to B within the chromite stability field, and will crystallize chromite until the melt composition reaches point B' on the olivine-chromite cotectic. 2) *The melt-rock reaction model*: primary magma A reacts with country-rock peridotite due to chemical and thermal disequilibrium. Addition of silica derived from incongruent melting of peridotite shifts the magma composition A to composition X, along the melt-rock-reaction line. The new melt X lies inside the chromite stability field and will crystallize chromite until the melt composition reaches point Y on the olivine-chromite cotectic.

type FeO/MgO (0.95), similar to melts derived from MOR peridotite. In contrast, the melt in equilibrium with CHR-2 had Al_2O_3, TiO_2, and FeO/MgO consistent with intra-plate picritic tholeiites (e.g., West Greenland). Such a contrasting geochemical signature cannot have resulted from the differentiation of a single melt. It rather reflects multiple intrusions of melts derived from chemically different sources, evolving during initial breakup of the continental lithosphere. This model apparently agrees with the idea that the Nurali ophiolite formed in a rifted continental margin, probably during the early stages of ocean opening (Fershtater et al., 1998; Zaccarini et al., 2004b; Dilek and Furnes, 2011). Under these geodynamic conditions, sub-continental mantle provided the floor for supra-Moho accumulation of layered sequences generated by successive intrusion of different melts derived from an almost undepleted subcontinental lithospheric mantle or the underlaying, upwelling asthenosphere.

Podiform chromitites in Ural-Alaskan complexes

The concentrically-zoned Alaskan-type complexes of the Urals are believed to have been emplaced as sub-vertical pipe-like bodies, into the gabbro-diorite of the Tagil island-arc zone. Rock petrography, trace element geochemistry and mineral chemistry suggest that the Ural-Alaskan-type intrusions were derived from crystallization of compositionally similar hydrous-mafic magmas with a high-K calc-alkaline affinity (Fershtater et al., 1997; Krause et al., 2007). Fractional crystallization and flow differentiation during ascent through sub-vertical conduits might be responsible for the concentric zoning (Murray, 1972). The variable proportions of dunite, wehrlite, clinopyroxenite, gabbro, and hornblendite, displayed by different complexes (Fig. 8) can be explained assuming that they are sections at different depths of structurally similar pipe-like bodies (Fershtater et al., 1999). Geobarometric data apparently support this conclusion, indicating a consistent increase of the crystallization pressure from ~ 2 kb in the gabbro-hornblendite-dominated intrusions (e.g., Sukhogor) trough 3-5 kb in clinopyroxenite-hornblendite-gabbro assemblages (e.g., Serebryanka, Kachkanar) to 7-10 kb in the predominantly dunite-wehrlite-clinopyroxenite bodies (Kytlym-Kosva Mt., Nizhny Tagil) representing the deep core of intrusive pipes (Fershtater and Pushkarev, 1990; Fershtater et al., 1999).

By analogy with similarly zoned complexes in Canada, Alaska and Kamchatka, they have been believed to be feeder pipes for andesitic volcanoes with the mafic and ultramafic rocks being cumulates and andesite lava the complementary liquid fractions (Taylor, 1967; Murray, 1972; Himmelberg and Loney, 1995). Alternatively, they might be the products of fractional crystallization of ankaramitic magmas (Irvine, 1973; Krause et al., 2007). The similarity with spinels from ankaramitic lavas supports this conclusion.

Syngenetic chromitite formed as an integral part of the dunite crystallization process, as indicated by their textural and compositional relationships with the host dunite (Garuti et al., 2003). During crystallization of dunite (T > 1300°C, P > 10 kb), the liquid composition was repeatedly shifted into the chromite stability field leading to the formation of small-sized chromitite bodies. This was possible due to periodic influxes of primitive magma having olivine and chromite on the liquidus, which could mix with an evolved hydrous fluid resident interstitial to partially crystallized dunite (Pushkarev and Anikina, 2002; Pushkarev et al., 2007; Krause et al., 2007).

Epigenetic chromitite veins and breccias of Nizhny Tagil formed by reaction of hydrous, alkali-rich fluids with semi-solid dunite at 800-700°C (Pushkarev and Anikina, 2002; Pushkarev et al., 2007). Chromite-olivine equilibration continued down to temperatures as low as 535°C. Water emanating from the epigenetic veins diffused through the wall rock dunite causing hydration of olivine and formation of thin serpentinite rims.

The origin of chromitite in the Butyrin vein of Kytlym is problematic. The process would have occurred at temperatures of 1000-950°C by reaction of dunite with a fluid-rich gabbroic melt of an uncertain provenance (Zaccarini et al., 2011). The calculated melt in equilibrium with the Butyrin vein chromite is not fully consistent with an arc affinity, but shows an extremely high TiO_2 content and FeO/MgO ratio, having an analogy with Fe-rich spinels from intraplate basalts and chromites from the Bushveld pipes (Table 7, Fig. 20B, C). This analogy might imply late infiltration of an exotic gabbroic melt into the Kytlym pipe, maybe during Late-Paleozoic plate collision. We note, however, that Fe-Ti-rich, hydrous melts resulting in the crystallization of magnetite-bearing amphibole-gabbros and hornblendite normally represent the final stage of solidification of Ural-Alaskan magmas. If such evolved melts had the chance to infiltrate into the outer part of the solid dunite-chromite cores, during the latest stage of emplacement, they could easily have reacted with the ultramafic rocks, producing mineral assemblages similar to that of the Butyrin vein, with orthopyroxene rims and Fe-Ti-rich chromite.

Stratiform chromitites in the East Khabarny layered sequence

The composition of chromite from chromitites of East-Khabarny overlap the field of Ural-Alaskan-type complexes, showing similar trends of $Cr\text{-}Al\text{-}Fe^{3+}$ and $Mg\text{-}Fe^{2+}$ substitution as well as Al_2O_3-TiO_2 relationships. Consistently, a strong similarity is observed between the calculated melts in equilibrium with the two types of chromitites. The data obtained support the conclusion based on bulk-rock geochemistry that the East-Khabarny layered sequence possibly derived from fractional crystallization of a high-Mg hydrous magma of the Ural-Alaskan type (Fershtater et al., 1997). The Early Devonian age proposed for the latest stage of emplacement of the East Khabarny complex coincides with that of the intrusion of the calc-alkalic Molostovsky complex, and other Ural-Alaskan complexes, e.g., the Kachkanar-Svetlyi Bor and Kytlym (Gottman et al., 2011, and references therein). Thus, several lines of evidence point to consanguinity between the parental magmas of the East-Khabarny and Ural-Alaskan complexes, although the lack of concentric zoning and the close association with ophiolitic residual mantle are apparently at odds. The un-conventional geological setting of the East-Khabarny layered sequence suggests that an Ural-Alaskan-type magma formed in a deep mantle section, below the Khabarny mantle harzburgite, could not reach the root zone of the Silurian island arc but was collected in a pond and fractionated at a mantle depth.

SUMMARY AND CONCLUSION

The chromitites of the Urals can be divided into four compositional groups corresponding to different parental melts and geodynamic environment of formation:

1) **The high-Al, low-Ti suite** (Al_2O_3 > 20 wt%, Cr# < 0.70, av. TiO_2 = 0.15 wt%, av. Fe^{3+}# = 0.05, δ logf(O_2) = -0.1 to +2.3) includes most of the supra-Moho stratiform chromitites (Kempirsai, Ray-Iz, Voykar-Syninsky, Nurali CHR-1), and some podiform chromitites hosted by ophiolitic mantle rocks (Voykar Syninsky, East Tagil, and Alapaevskoy). Chromite deposits of this type are of a sub-economic size. They crystallized from MORB-type tholeiitic magmas (av. FeO/MgO = 1.0) produced by low degrees of melting of a slightly depleted source during Ordovician-Early Devonian extension (Savelieva et al., 2007). Favorable geodynamic settings were subduction-unrelated environments such as: i) mid-oceanic ridges, ii) rifted continental margins, and iii) back-arc basins (Paktunq, 1990; Leblanc and Nicolas, 1992; Zhou and Robinson, 1997; Proenza et al., 1999; Rollinson, 2008).

2) **The high-Al, high-Ti suite** (Al_2O_3 > 20 wt%, Cr# < 0.70, av. TiO_2 = 0.80 wt%, av. Fe^{3+}# = 0.20) is represented by the CHR-2 supra-Moho chromitite layer of Nurali. This chromitite is rather unusual showing Al_2O_3-TiO_2 relationships comparable with chromitites from continental layered intrusions. The calculated melt in equilibrium with chromite differs from MORB for its extremely high iron content (av. FeO/MgO = 1.90), while the chromite displays higher Fe^{3+}# compared with CHR-1, indicating an increased oxidation state of the parental melt. These chemical features are broadly consistent with those of transitional tholeiites. Coexistence of chromitites with such a bimodal compositional character in the Nurali cumulate sequence is interpreted as a feature typical of continental margin (CM) ophiolite complexes.

3) **The high-Cr, low-Ti suite** (Cr# > 0.70, Al_2O_3 < 20 wt%, TiO_2 < 0.30 wt%, av. Fe^{3+}# = 0.06, δlogf(O_2) = -1.7 to +2.7) includes most podiform chromitites hosted by the ophiolitic mantle rocks and only two examples of supra-Moho stratiform chromitites. They have relatively low FeO/MgO, were crystallized from high-Mg magmas with average compositions referable to picritic tholeiite or boninite (FeO/MgO < 1.0). These melts were produced during an eastward intra-oceanic subduction driven by Devonian compression, which was active from the Polar to the Southern Urals (Melcher et al., 1999; Savelieva et al., 2007). High degrees of partial melting were induced in the SSZ mantle wedges by fluids emanating from the subducting slabs. Large volumes of boninite-type melts were injected upwards into high permeability channels. Extensive chromite precipitation took place in the channels forming essentially discordant deposits. As it happens in other chrome provinces, precipitation of chromitite resulted from reaction between the adiabatically ascending melts and the wall-rock residual mantle (Zhou and Robinson, 1994; Arai, 1997; Robinson et al., 1997; Proenza et al., 1999; Rollinson, 2008). Strong thermal gradients, prolonged melt flow (Leblanc and Nicolas, 1992), and high melt/wall-rock chemical disequilibrium (Zhou and Robinson, 1997) were critical factors for the formation of giant deposits of metallurgic-grade chromite in the ophiolites of the Urals (Kempirsai, Kraka, Ray-Iz, Voykar-Syninsky). The Urals represent a typical case for large, high-Cr chromite deposits being "*a marginal-basin phenomenon*" (Roberts, 1988), apparently restricted to SSZ-type ophiolites (Dilek and Furnes, 2011).

4) **The high-Cr, high-Ti suite** (Cr# > 0.70, Al_2O_3 < 20 wt%, TiO_2 = 0.38-1.30 wt%, Fe^{3+}# = 0.20-1.29, δlogf(O_2) = +0.9 to +5.9) is represented by chromitites from the Ural-Alaskan intrusions and the East-Khabarny complex. They have crystallized from Fe-rich magma (FeO/MgO > 1) under high oxygen fugacity conditions. The melt is characterized by a high-Ti, high-K, calc-alkaline affinity and was generated by partial melting of a fluid-metasomatized mantle source (Garuti et al., 1997; 2003; Fershtater et al., 1999). Formation of these complexes in the Urals appear to have occurred periodically, from Late Neo-Proterozoic, to Ordovician-Silurian, and Early Devonian (Savelieva et al., 2007; Gottman et al., 2011; and references therein). Chromitite formed in a sequence of events from syngenetic to epigenetic with respect to the crystallization of dunite, triggered by a sort of "deuteric" reaction with: i) residual fluids, after partial to total crystallization of olivine (Pushkarev and Anikina, 2002; Pushkarev et al., 2007), or ii) evolved gabbroic melts possibly derived from differentiation of the Ural-Alaskan magma itself (Zaccarini et al., 2011).

The proposed tectonic setting would indicate preferential location of Ural-Alaskan type intrusions at convergent plates, in subduction-influenced arc settings. However, the chromitites are similar to chromitites in the zoned complexes of Galmoenan (Kamchatka island arc) and Kondyor (Russian Far East craton), and have characteristics in common with those in continental layered intrusions (e.g., the Bushveld pipes). The analogy with the zoned ultramafic complex intruded into the Asian continental craton (e.g., Kondyor), several hundred kilometers far away from subducting plates, poses the question of the true tectonic setting for the generation of Ural-Alaskan magmas. The present data suggest that formation of Ural-Alaskan type complexes is not restricted to SSZ, island-arc regions, but can take place in a wider spectrum of geodynamic settings than generally thought. This fact may indicate the involvement of deep asthenospheric sources in their generation.

ACKNOWLEDGEMENTS

We wish to thank the two referees, Eero Hanski and Paolo Nimis, for their constructive criticisms that significantly improved the quality of the manuscript. Thanks are due to the editor Riccardo Tribuzio and the executive editor Luca Pandolfi for the editorial management. The University Centrum for Applied Geosciences (UCAG), Austria, is acknowledged for making available the facilities of the E.F. Stumpfl Electron Microprobe Laboratory at the University of Leoben. Many thanks to the project N° 12-c-5-1004 Ural Division of RAS.

REFERENCES

Arai S., 1980. Dunite-harzburgite-chromitite complexes as refractory residue in the Sangun-Yamaguchi zone, western Japan. J. Petrol., 21: 141-165.

Arai S., 1992. Chemistry of chromian spinel in volcanic rocks as a potential guide to magma chemistry. Mineral. Mag., 56: 173-184.

Arai S., 1997. Origin of podiform chromitites. J. Asian Earth Sci., 15: 303-310.

Augé T., 1987. Chromite deposits in the northern Oman ophiolite: Mineralogical constraits. Mineral. Dep., 22: 1-10.

Augé T., Genna A., Legendre O., Ivanov K.S. and Volchenko Y.A., 2005. Primary platinum mineralization in the Nizhny Tagil and Kachkanar ultramafic complexes, Urals, Russia: A genetic model for PGE concentration in chromite-richzones. Econ. Geol., 100: 707-732.

Ballhaus C., Berry R.F. and Green D.H., 1991. High-pressure experimental calibration of the olivine-orthopyroxene-spinel geobarometer: implications for the oxidation state of the upper mantle. Contrib. Mineral. Petrol., 107: 27-40.

Barnes S.J. and Roeder P.L., 2001. The range of spinel compositions in terrestrial mafic and ultramafic rocks. J. Petrol., 42: 2279-2302.

Bédard J., 1989. Disequilibrium mantle melting. Earth Planet. Sci. Lett., 91: 359-366.

Betekhtin A.G., 1961. Mikroskopische Untersuchungen an Platinerzen aus dem Ural. N. Jb. Miner. Abh., 97: 1-34.

Chashchukhin I.S., Votyakov S.L., Uimin S.G., Borisov D.R. and Bikov V.N., 1996. Mössbauer spectroscopy of chrome spinels and problems of oxygen termo-barometry in chromite-bearing ultramafics of the Urals. Inst. Geol. Geochem., Ekaterinburg, 136 pp. (in Russian).

Chashchukhin I.S., Votyakov S.L. and Uimin S.G., 1998. Oxygen thermometry and barometry in chromite-bearing ultramafic rocks: an exmple of ultramafic massifs on the Urals. II. Oxidation state of ultramafics and the composition of mineralizing fluids. Geochem. Int., 36: 783-791.

Chashchukhin I.S., Votyakov S.L., Pushkarev E.V., Anikina E.V., Mironov A.B. and Uimin S.G., 2002. Oxythermobarometry of ultramafic rocks from the Ural Platiniferous Belt. Geochemistry, 8: 846-863. (in Russian).

Chashchukhin I.S., Votyakov S.L. and Scianova Yu.V., 2007. Crystal chemistry of chrome spinel and oxygen thermobarometry in ultramafic rocks. Russian Ackad. Sci., Ural division, Inst. Geol. Geochem., Ekaterinburg, 312 pp. (in Russian)

Crawford A.J., Falloon T.J. and Green D.H., 1989: Classification, petrogenesis and tectonic setting of boninites. In: A.J. Crawford (Ed.), Boninites. Unwin Hyman, London, p. 1-49.

Dick H.J.B. and Bullen T., 1984. Chromian spinel as a petrogentic indicator in abyssal and alpine-type peridotites and spatially associated lavas. Contrib. Mineral. Petrol., 86: 54-76.

Dickey J.S. Jr., 1975. A hypothesis of origin for podiform chromite deposits. Geochim. Cosmochim. Acta, 39: 1061-1074.

Dilek Y. and Furnes H., 2011. Ophiolite genesis and global tectonics: Geochemical and tectonic fingerprinting of ancient oceanic lithosphere. Geol. Soc. Am. Bull., 123: 387-411.

Duparc L. and Tikonowitch M.N., 1920. Le platine et le gîtes platinifères de l'Oural et du monde. Soc. Anon. Éd. Son., Rue du Stand 46, Genève, 546 pp.

Economou-Eliopoulos M. and Zhelyaskova-Panayotova M., 1998. Comparative study of the geochemistry of chromite ores from the Kempirsai (Urals) and Rhodope (Balkan Peninsula) ophiolitic massifs. Bull. Geol. Soc. Greece, 32 (3): 203-211.

Efimov A.A. and Tavrin I.F., 1978. On the genetic similarity between platinum-bearing dunites of the Urals and those of the Aldan Shield. Dokl. Earth Sci., 243: 991-994.

Efimov A.A., Efimova L.P. and Maegov V.I., 1993. The tectonics of the Platinum-bearing belt of the Urals: Composition and mechanism of structural development. Geotectonics, 27: 197-207.

Efimov A.A., Lennykh V.I., Puchkov V.N., Saveliev A.A., Savelyeva G.N. and Jaseva R.G., 1978. Guidebook for excursion, ophiolites of Polar Urals. In: N. Bogdanov (Ed.), 4th Field Conference. Mosckow, August 1-15, 1978.

Elburg M.A., Kamenetsky V.S., Foden J.D. and Sobolev A., 2007. The origin of medium-K ankaramitic arc magmas from Lomboc (Sunda arc, Indonesia): mineral and melt inclusion evidence. Chem. Geol., 240: 260-279.

Escayola M., Garuti G., Zaccarini F., Proenza J.A., Bédard J.H., and Van Staal C., 2011. Chromitite and platinum-group-element mineralization at Middle Arm Brook, Central Advocate ophiolite complex, Baie Verte Peninsula, New Foundland, Canada. Can. Mineral., 49: 1561-1585.

Evans B.W. and Frost B.R., 1975. Chrome-spinel I progressive metamorphism - a preliminary analysis. Geochim. Cosmochim. Acta, 39: 959-972.

Falloon T.J. and Danyushevsky L.V., 2000. Melting of refractory mantle at 1.5, 2.0 and 2.5 GPa under anhydrous and H_2O undersaturated conditions: implications for the petrognesis of high-Ca boninites and the influence of subduction components on mantle melting. J. Petrol., 41: 257-283.

Ferrario A. and Garuti G., 1988. Platinum-group minerals in chromite-rich horizons of the Niquelandia Complex (Central Goias, Brazil). In: H.M. Prichard, P.J. Potts, J.F.W. Bowels and S.J. Cribb (Eds.), Geo-Platinum 87, Proceed. Symp. Geo-Platinum '87, Apr. 1987, Open Univ., Milton Keynes, U.K., p. 261-272.

Fershtater G.B. and Pushkarev E.V., 1990. Subvolcanic ultramafites of the Ural Platinum Belt. Zap. Vses. Mineral. O-va, 1/119: 51-62 (in Russian).

Fershtater G.B. and Pushkarev E.V., 1991. The dunite-clinopyroxenite-gabbro formation in the East Khabarny massif. In: G.B Fershtater and A.P. Krivenko (Eds.), Petrology of post-harzburgite intrusives in the Kempirsai and Khabarny ophiolite association. Ural Branch Nat. Acad. Sci. USSR, Sverdlovsk, p. 81-152. (in Russian)

Fershtater G.B., Bea F., Borodina N.S. and Montero P., 1998. Lateral zonation, evolution, and geodynamic interpretation of magmatism of the Urals: new petrological and geochemical data. Petrology, 6: 451-433.

Fershtater G.B., Montero P., Borodina N.S., Pushkarev E.V., Smirnov V.N. and Bea F., 1997. Uralian magmatism: an overview. Tectonophysics, 276: 87-102.

Fershtater G.B., Bea F., Pushkarev E.V., Garuti G., Montero P. and Zaccarini F., 1999. Insight into the petrogenesis of the Urals Platinum Belt: New geochemical evidence. Geochem. Intern., 37: 302-319.

Garuti G., 2004. Chromite-platinum-group element magmatic deposits. In: De B.Vivo et al. (Eds.), Geology, Encyclopedia of Life Support Systems (EOLSS). UNESCO, Eolss Publisher, Oxford, UK [http://www.eolss.net].

Garuti G., Pushkarev E. and Zaccarini F., 2002. Composition and paragenesis of Pt-alloys from chromitites of the Ural-Alaskan type Kytlym and Uktus Complexes, Northern and Central Urals, Russia. Can. Mineral., 40: 1127-1146.

Garuti G., Proenza J.A. and Zaccarini F., 2007. Distribution and mineralogy of platinum-group elements in altered chromitites of the Campo Formoso layered intrusion (Bahia State, Brazil): control by magmatic and hydrothermal processes. Mineral. Petrol., 86: 159-188.

Garuti G., Zaccarini F., Moloshag V. and Alimov V., 1999. Platinum-group minerals as indicators of sulfur fugacity in ophiolitic upper mantle: an example from chromitites of the Ray-Iz ultramafic complex (Polar Urals, Russia). Can. Mineral., 37: 1099-1116.

Garuti G., Pushkarev E., Zaccarini F., Cabella R. and Anikina E., 2003. Chromite composition and platinum-group mineral assemblage in the Uktus Uralian-Alaskan-type complex (Central Urals, Russia). Mineral. Dep., 38: 312-326.

Garuti G., Fershtater G.B., Bea F., Montero P., Pushkarev E. and Zaccarini F., 1997. Platinum-group elements as petrological indicators in mafic-ultramafic complexes of the Central and Southern Urals. Tectonophysics, 276: 181-194.

Gervilla F. and Leblanc M., 1990. Magmatic ores in high-temperature alpine-type lherzolite massifs (Ronda, Spain and Beni Bousera, Morocco). Econ. Geol., 85: 112-132.

Gottman I.A., Pushkarev E.V. and Kudryoshov N.M., 2011. The upper geochronological limit for dunites of the East-Khabarnyi gabbro-ultramafic complex (South Urals) by the data of U-Pb age of zircons extracted from vein hornblendites. Geology, 438: 593-597.

Grieco G., Diella V., Chaplygina N.L. and Savelieva G.N., 2007. Platinum-group elements zoning and mineralogy of chromitites from the cumulate sequence of the Nurali massif (Southern Urals, Russia). Ore Geol. Rev., 30: 257-276.

Hill R. and Roeder P., 1974. The crystallization of spinel from basaltic liquid as a function of oxygen fugacity. J. Geol., 82: 709-729.

Himmelberg R.G. and Loney R.A., 1995. Characteristics and petrogenesis of Alaskan-type ultramafic-mafic intrusions, southeastern Alaska. U.S. Geol. Surv. Prof. Pap., 1564: 1-47.

Irvine T.N., 1965. Chromian spinel as a petrogenetic indicator. Part 1. Theory. Can. J. Earth Sci., 2: 648-672.

Irvine T.N., 1967. Chromian spinel as a petrogenetic indicator. Part 2. Petrologic applications. Can. J. Earth Sci., 4: 71-103.

Irvine T.N., 1973. Bridget Cove volcanics, Juneau Area, Alaska: possible parental magma of Alaskan-type ultramafic complexes. Carn. Inst. Wash. Yearb., 72: 478-491.

Irvine T.N., 1977a. Chromite crystallization in the join Mg_2SiO_4-$CaMgSi_2O_6$-$CaAl_2Si_2O_8$-$MgCr_2O_4$-SiO_2. Carn. Inst. Wash. Yearb., 76: 465-472.

Irvine T.N., 1977b. Origin of chromite layers in the Muskox intrusion and other intrusions: A new interpretation. Geology, 5: 273-277.

Ivanov O.K., 1997. Concentrically zoned pyroxenite-dunite massifs of the Urals: (Mineralogy, petrography, genesis). Ekaterinburg. Publ. House Urals Univ., 488 pp. (in Russian)

Ivanov S.N. and Rusin A.I., 1986. Model for the evolution of the linear fold belt in the continents: example of the Urals. Tectonophysics, 127: 383-397.

Johan Z., 2002. Alaskan-type complexes and their Platinum-group element mineralization. In: L.J. Cabri (Ed.), The geology, geochemistry, mineralogy and mineral beneficiation of Platinum-group elements, C.I.M.M., Spec. Vol., 54: 669-719.

Kamenetsky V.S., Crawford A.J. and Meffre S., 2001. Factors controlling chemistry of magmatic spinel: an empirical study of associated olivine, Cr-spinel and melt inclusions from primitive rocks. J. Petrol., 42: 655-671.

Koroteev V.A., De Boorder H., Necheukhin V.M. and Sazonov V.N., 1997. Geodynamic setting of the mineral deposits of the Urals. Tectonophysics, 276: 291-300.

Krause J., Brügmann G.E. and Pushkarev E.V., 2007. Accessory and rock forming minerals monitoring the evolution of zoned mafic-ultramafic complexes in the Central Ural Mountains. Lithos, 95: 19-42

Krause J., Brügmann G.E. and Pushkarev E.V., 2011. Chemical composition of spinel from Uralian-Alaskan-type mafic-ultramafic complexes and its petrogenetic significance. Contrib. Mineral. Petrol., 161: 255-273.

Kravchenko G.G., 1986a. The Urals chromite deposits. In: B. Carter et al. (Eds.), Metallogeny of basic and ultrabasic rocks (Regional Presentation). Theophrastus Publ., Athens, p. 179-187.

Kravchenko G.G., 1986b. Geological position and structure of chromite deposits in the Ural mountains. In: W. Petrascheck et al. (Eds.), Chromitites, UNESCO's IGCP-197 project, Metallogeny of Ophiolites. Theophrastus Publ., Athens, 3-21.

Kravchenko G.G. and Grigoryeva I.I., 1986. The Kempirsai chromite-bearing massif in the Ural mountains. In: W. Petrascheck et al. (Eds.), Chromitites, UNESCO's IGCP-197 project, Metallogeny of Ophiolites. Theophrastus Publ., Athens, 23-44.

Larsen L.M. and Pedersen A.K., 2009. Petrology of the Paleocene picrites and flood basalts on Disko and Nuussuaq, West Greenland. J. Petrol., 50: 1667-1711.

Lago B.L., Rabinowicz M. and Nicolas A., 1982. Podiform chromite ore bodies: a genetic model. J. Petrol., 23: 103-125.

Leblanc M. and Nicolas A., 1992. Ophiolitic chromitites. Int. Geol. Rev., 34: 653-686.

Maurel C., 1984. Etude expérimentale de l'équilibre spinelle chromifère liquide silicaté basique. SFMC Meet. "Les spinelles", Lille, oral. comm.

Maurel C. and Maurel P., 1982. Etude expérimentale de la distribution de l'aluminium entre bain silicaté basique et spinel chromifère. Implications pétrogénétiques: teneur en chrome des spinelles. Bull. Mineral. 105: 197-202 (in French).

Melcher F., Stumpfl E.F. and Distler V., 1994. Chromite deposits of the Kempirsai massif, Southern Urals, Kazakhstan. Trans. IMM, 103, Sect. B: 107-120.

Melcher F., Grum W., Simon G., Thalhammer T.V. and Stumpfl E.F., 1997. Petrogenesis of the ophiolitic giant chromite deposits of Kempirsai, Kazakhstan: a study of solid and fluid inclusions in chromite. J. Petrol., 38: 1419-1458.

Melcher F., Grum W., Thalhammer T.V. and Thalhammer O.A.R., 1999. The giant chromite deposits at Kempirsai, Urals: constraints from trace element (PGE, REE) and isotope data. Mineral. Dep., 34: 250-272.

Moloshag V.P. and Smirnov S.V., 1996. Platinum mineralization of the Nurali mafic-ultramafic massif (Southern Urals). Notes of the Russian Mineralogical Society. Part 125 (1): 48-54 (in Russian).

Murray C.G., 1972. Zoned ultramafic complexes of the Alaskan-type: feeder pipes of andesitic volcanoes. Mem. Geol. Soc. Am., 132: 313-335.

Mussalam K., Jung D. and Burgath K., 1981. Textural features and chemical characteristics of chromitites in ultramafic rocks, Chalchidiki Complex (Northeastern Greece). TMPM, 29: 75-101.

Ortiz-Hernandez L.E., 2000. An arc ankaramite occurrence in central Mexico. Rev. Mex. Cien. Geol., 17: 34-44.

Ozawa K., 1984. Olivine-spinel geospeedometry: analysis of diffusion-controlled Mg-Fe^{2+} exchange. Geochim. Cosmochim. Acta, 48: 2597-2611.

Paktunq A.D., 1990. Origin of podiform chromite deposits by multistage melting, melt segregation and magma mixing in the upper mantle. Ore Geol. Rev. 5: 211-222.

Pavlov N.V. and Grigoryeva I.I., 1977. Deposits of chromium. In: V.I. Smirnov (Ed.), Ore deposits of the USSR. Pitman London, 1: 179-236.

Perevozchikov B.V. and Puchkov V.N., 1990. Geologic structure of the massif. In: V.N. Puchkov and D.S. Steinberg (Eds.), Structure, evolution and minerogenesis of the Ray-Iz Ultramafic Massif. Ural Branch Nat. Acad, Sci. USSR, Sverdlovsk, p. 19-28. (in Russian)

Perevozchikov B.V., Alimov V.Yu., Tsaritsin Ye.P., Chashchukhin I.S. and Sherstobitova L.A., 1990. Chrome spinels and chromite ore deposits of the massif. In: V.N. Puchkov and D.S. Steinberg (Eds.), Structure, evolution and minerogenesis of the Ray-Iz Ultramafic Massif. Ural Branch Nat. Acad. Sci. USSR, Sverdlovsk, p. 149-194 (in Russian).

Pérez-Estuan A. and Brown D., 1996. Uralides: A key to understanding collisional orogeny. In: D.G. Gee and H.J. Zeyen (Eds.), Europrobe 1996 - Lithosphere dynamics: Origin and evolution of continents. Europrobe Secretariate, Upsala Univ., p. 28-39.

Pertsev A.N., Spadea P., Savelieva G.N. and Gaggero L., 1997. Nature of the transition zone in the Nurali ophiolite, Southern Urals. Tectonophysics, 276: 163-180.

Proenza J.A., Gervilla F., Melgarejo J.C. and Bodinier J.L., 1999. High-Al and High-Cr chromitites from the Mayarí-Baracoa ophiolitic belt (eastern Cuba): consequence of interaction between volatile-rich melts and peridotites in suparasubduction mantle. Econ. Geol., 94: 547-566.

Pushkarev E.V., 2000. Petrology of the Uktus dunite-clinopyroxenite-gabbro massif (the Middle Urals). Monography Russian Acad. Sci. Ural Branch, Inst. Geol. Geochem. Ekaterinburg. (in Russian)

Pushkarev E.V. and Anikina E.V., 2002. Low temperature origin of the Ural-Alaskan type platinum deposits: Mineralogical and geochemical evidence. In: A. Boudreau (Ed.), 9th Intern. Platinum Symp., July 2002, Billings, Montana (USA), Extended Abstr., p. 387-390.

Pushkarev E.V., Anikina E.V., Garuti G. and Zaccarini F., 2007. Chromium-Platinum deposits of Nizhny-Tagil type in the Urals: structural-substantial characteristic and a problem of genesis. Litosfera, 3: 28-65 (in Russian)

Pushkarev E.V., Anikina E.V., Garuti G., Zaccarini F. and Cabella R., 1999. Geikielite (Mg-ilmenite) in association with Cr-spinel and platinoids from the Uktus massif dunite, Middle Urals: genetic implications. Dokl. Earth Sci., 369 A9: 1220-1223.

Razin L.V., 1976. Geologic and genetic features of forsterite dunites and their platinum-group mineralization. Econ. Geol., 71: 1371-1376.

Roberts S., 1988. Ophiolitic chromitite formation: a marginal basin phenomenon? Econ. Geol., 83: 1034-1036.

Robinson P.T., Zhou M.F., Malpas J. and Bai W.J., 1997. Podiform chromitites: Their composition, origin and environmental formation. Episodes, 20: 247-252.

Roeder P.L., 1994. Chromite: From the fiery rain of chondrules to the Kilauea Iki lava lake. Can. Mineral., 22: 729-746.

Roeder P.L. and Reynolds I., 1991. Crystallization of chromite and chromium solubility in basaltic melts. J. Petrol., 32: 909-934.

Rollinson H., 2008. The geochemistry of mantle chromitites from the northern part of the Oman ophiolite: inferred parental melt compositions. Contrib. Mineral. Petrol., 156: 273-288.

Saveliev A.A., 1977. Chromitites of the Voykar-Sininsky massif. In: Genesis of ultramafites and related ores. Inst. Geol. Geochem., Sverdlovsk, p. 63-77 (in Russian)

Saveliev A.A. and Savelieva G.N., 1991. The ophiolites of the Kempirsai massif: basic features of their structural and compositional evolution. Geotectonics, 15: 498-511.

Savelieva G.N., 1987. Gabbro-ultramafic complexes in the Urals and their equivalents in the modern oceanic crust. Nauka, Moscow, 245 pp. (in Russian).

Savelieva G.N., 2004. Chromitites of the Polar Urals, Russia. In: Proceed. 8th ICAM-BR on Applied Mineralogy, San Paulo 2004, 2: 943-945.

Savelieva G.N. and Saveliev A.A., 1991. Chromite in the ophiolite sequence. Geotectonica, 2: 47-58 (in Russian).

Savelieva G.N. and Saveliev A.A., 1992. Relationship between peridotites and gabbroic sequences in the ophiolites of the Urals and the lesser Caucasus. Ofioliti, 17: 117-138.

Savelieva G.N., Suslov P.V. and Larionov A.N., 2007. Vendian tectono-magmatic events in the Mantle ophiolitic complexes of the Polar Urals: U-Pb dating of zircons from chromitite. Geotectonics, 41: 105-113.

Savelieva G.N., Sharaskin A.Yu., Saveliev A.A, Spadea P. and Gaggero L., 1997. Ophiolites of the southern Uralides adjacent to the East European continental margin. Tectonophysics, 276: 117-137.

Spadea P. and D'Antonio M., 2006. Initiation and evolution of intraoceanic subduction in the Uralides: Geochemical and isotopic constraints from Devonian oceanic rocks of the Southern Urals, Russia. Island Arc, 15: 7-25.

Stowe C.W., 1987. Evolution of chromium ore fields. Van Nostrund Reinhold, New York, 340 pp.

Stowe C.W., 1994. Composition and tectonic settings of chromite deposits through time. Econ. Geol., 89: 528-546.

Taylor H.P. Jr., 1967. The zoned ultramaphic complexes of southern Alaska. In: PJ Wyllie (Ed.), Ultramafic and related rocks. John Wiley and Sons, Inc, New York. p 97-121.

Thalhammer T.V., 1996. The Kempirsai ophiolite complex, south Urals. Petrology, geochemistry, platinum-group minerals, chromite deposits. Unpubl. Ph.D. thesis, Univ. Leoben, 196 pp.

Thayer T.P., 1970. Chromite segregations as petrogenetic indicators. In: Symposium on the Bushveld igneous complex and other layered intrusions, Geol. Soc. South Africa Spec. Publ., 1: 380-390.

Ukhanov A.V., Nikolaskaya N.Ye. and Guzkova A.V., 1990. Traces of differential crystallization in Ural chromites. Geokhimia, 1: 61-72.

Ulmer P., 1989. The dependence of the Fe^{2+}-Mg cation-partitioning between olivine and basaltic liquid on pressure, temperature and composition. Contrib. Mineral. Petrol., 101: 261-273.

Uysal I., Sadiklar M.B., Zaccarini F., Garuti G., Tarkian M. and Meisel T., 2010. Cr-PGE mineralization in the Turkish ophiolites: the state of the art. 11th Platinum Symp., Sudbury, Jun. 2010, Abstr. Vol., Ontario Geological Survey, Miscellaneous release-data, p. 269.

Uysal I., Tarkian M., Sadiklar M.B., Zaccarini F., Meisel T., Garuti G. and Heidrich S., 2009. Petrology of high-Cr and high-Al ophiolitic chromitites from the Muğla, SW Turkey: implications from composition of chromite, solid inclusions of platinum-group minerals, silicate, and base metal mineral, and Os-isotope geochemistry. Contrib. Mineral. Petrol., 158: 659-674.

Zaccarini F., 2005. Composition of chromitites and associated solid inclusions: a key to understanding mantle and derived magmas. Doctoral Thesis, Univ. Modena and Reggio Emilia, Italy, 86 pp. (in Italian)

Zaccarini F., Pushkarev E. and Garuti G., 2008. Platinum-group element mineralogy and geochemistry of chromitite of the Kluchevskoy ophiolite complex, central Urals (Russia). Ore Geol. Rev., 33: 20-30.

Zaccarini F., Garuti G. and Cawthorn G., 2002. Platinum group minerals in chromitite xenoliths from the ultramafic pipes of Onverwacht and Tweefontein (Bushveld Complex). Can. Mineral., 40: 481-497.

Zaccarini F., Stumpfl E.F. and Garuti G., 2004a. Zirconolite and other Zr-Th-U minerals in chromitites of the Finero complex (Western Alps, Italy): evidence for carbonatite-type metasomatism in a subcontinental mantle plume. Can. Mineral., 42: 1825-1845.

Zaccarini F., Garuti G. and Pushkarev E.V., 2011. Unusually PGE-rich chromitite in the Butyrin vein of the Kytlym Uralian-Alaskan complex, Northern Urals, Russia. Can. Mineral., 49: 52-72.

Zaccarini F., Pushkarev E., Fershtater G.B. and Garuti G., 2004b. Composition and mineralogy of PGE-rich chromitites in the Nurali Lherzolite-gabbro complex, Southern Urals, Russia. Can. Mineral., 42: 545-562.

Zhou M.F. and Robinson P.T., 1994. High-Cr and high-Al podiform chromitites from western China: relationships to partial melting and melt/rock reaction in the upper mantle. Int. Geol. Rev., 36: 678-686.

Zhou M.F. and Robinson P.T., 1997. Origin and tectonic environment of podiform chromite deposits. Econ. Geol., 92: 259-262.

Zhou M.F. and Bai W.J. 1992. Chromite deposits in China and their origin. Mineral. Dep., 27: 192-199.

Zhou M.F., Robinson P.T. and Bai W.J. 1994. Formation of podiform chromitites by melt/rock interaction in the upper mantle. Mineral. Dep., 29: 98-101.

Zoloev K.K., Volchenko Yu.A., Koroteev V.A., Malakhov I.A., Mardirosyan A.N. and Khripov V.N., 2001. Platinum ores in different complexes of the Urals. Ural State Univ. Press, Ekaterinburg, 199 pp. (in Russian).

Received, February 21, 2012
Accepted, May 21, 2012